energies

MDPI

Review

Metal-Supported Solid Oxide Fuel Cells: A Review of Recent Developments and Problems

Serikzhan Opakhai * and Kairat Kuterbekov

Department of Physics and Technology, L.N. Gumilyov Eurasian National University, Astana 010000, Kazakhstan; kkuterbekov@gmail.com

* Correspondence: serikjan_0707@mail.ru

Abstract: The design of metal-supported solid oxide fuel cells (MS-SOFCs) has again aroused interest in recent years due to their low cost of materials, strength, and resistance to thermal cycling, as well as the advantages of manufacturability. MS-SOFCs are promising electrochemical devices for hydrogen energy. Compared to SOFCs, where ceramic electrodes or electrolytes are used as a carrier base, they are of great interest due to their fast start-up capability, greater reliability, mechanical stability, and resistance to the thermal cycle. MS-SOFCs have many advantages over conventional ceramic-based SOFCs, with the selection of metal-based electrode materials (anode, cathode) and their degradation processes being some of the biggest challenges facing researchers. Therefore, this review reports on the state of the latest research on MS-SOFCs with various structures, discusses the corresponding electrode materials and their existing problems, and puts forward topical issues that need to be addressed in MS-SOFCs.

Keywords: metal-supported solid oxide fuel cells; electrode; thermal expansion coefficient; substrate; materials; degradation

Citation: Opakhai, S.; Kuterbekov, K. Metal-Supported Solid Oxide Fuel Cells: A Review of Recent Developments and Problems. *Energies* **2023**, *16*, 4700. https://doi.org/10.3390/en16124700

Academic Editors: Muhammad Aziz and Vladislav A. Sadykov

Received: 24 April 2023
Revised: 18 May 2023
Accepted: 12 June 2023
Published: 14 June 2023

1. Introduction

Throughout the 20th century, society became increasingly dependent on fossil fuels as a source of energy for utilities, transportation, and a host of other sectors. Conventional methods of generating energy from fossil fuels have numerous inherent disadvantages, including high levels of pollution, low efficiency, and lack of renewable resources [1–3].

Electrochemical fuel cells, especially solid oxide fuel cells (SOFCs), are promising alternative energy conversion devices that have the potential to realize hydrocarbon neutrality and are compatible with existing infrastructure, allowing certain steps towards completely green fuels [4,5].

SOFCs are one of the most excellent fuel cell systems of particular interest due to the control of high operating temperatures and fuel management [6]. Similar to other types of fuel cells, SOFCs require fuel (hydrogen) and oxidizers such as oxygen to react electrochemically at high temperature and generate electrical energy. Hydrogen is typically the preferred fuel because of its high electrochemical activity. However, carbon monoxide can also be used as a fuel in conjunction with hydrogen. Additionally, when operating in the internal reforming mode, hydrocarbon gas can be directly used as a fuel [5]. Figure 1 illustrates the standard structure and operating principle of an SOFC.

As can be seen from Figure 1, an SOFC consists of three main components: a dense electrolyte, a porous anode, and a porous cathode [2]. An SOFC is a solid-state energy converter that directly converts the chemical energy of fuel (hydrogen, natural gas, etc.) into electrical energy through electrochemical reactions. It has great prospects for use in large power plants [3–5] due to its high efficiency, low emissions, and lack of noise.

However, SOFC power generation technology has not yet been developed for large-scale applications, and its main limitations are its cost and lifetime. The new design of the

metal support makes it possible to enhance the mechanical resistance of an individual cell, increase the thermal shock resistance of the battery, and reduce the cost of the SOFC system. As a result, in recent years, metal-based SOFCs (MS-SOFCs) have attracted wide global attention and have gradually become an area of SOFC research [7].

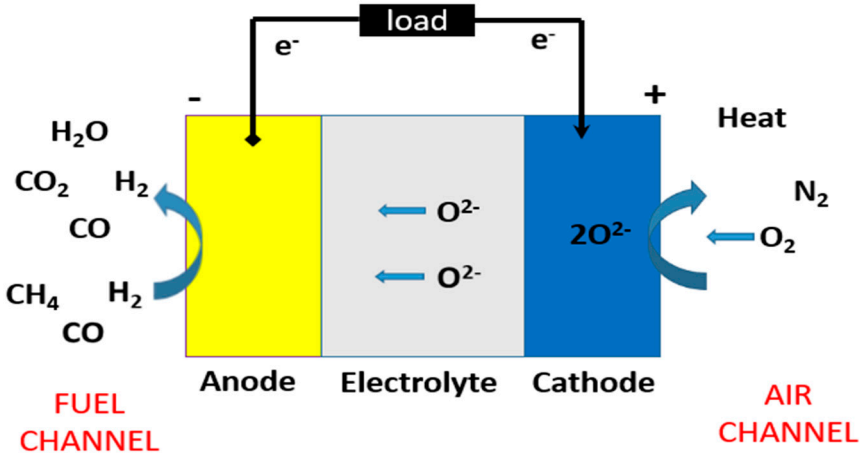

Figure 1. Typical structure and operating principle of SOFC.

Compared to traditional ceramic-supported structures, metal-supported SOFCs have the following advantages [8,9]:

(a) Low cost. The use of metal substrates can lower material costs compared to ceramic-supported SOFCs, which can require expensive materials such as yttria-stabilized zirconia (YSZ).
(b) Quick startup. The good thermal conductivity of the metal can make the MS-SOFC start up quickly, allowing it to be used in the mobile area.
(c) Manufacturability. Stainless steel metal has good ductility, which greatly reduces the complexity of SOFC processing.
(d) Ease of sealing. The use of proven technology for sealing metallic materials avoids the difficulties associated with sealing conventional SOFCs [9].

However, along with the aforementioned advantages, there are some issues with the development of MS-SOFCs. In this review, we extensively discuss the types of MS-SOFCs; anode, cathode, and electrolyte materials and their degradation processes; issues with the metal support; and finally, the future prospects and problems for the development of MS-SOFCs.

Types of MS-SOFCs

So far, two generations of flat cell SOFCs have been studied in the world with a significant improvement in performance: the first includes electrolyte-supported SOFCs (ES-SOFCs), and the second includes anode-supported (AS-SOFCs) and metal-supported SOFCs (MS-SOFCs) (Figure 2).

The commercialization of traditional SOFC technology faces significant challenges due to various reasons. These challenges include the high cost of raw materials, issues related to cell sealing, limited stress resistance of the cell under rapid thermal transients and mechanical shocks, susceptibility to anode oxidation, and difficulties in achieving high-yield production of large and intricate ceramic components. These factors contribute to the complexity and cost of scaling up traditional SOFC technology for commercial applications [10,11].

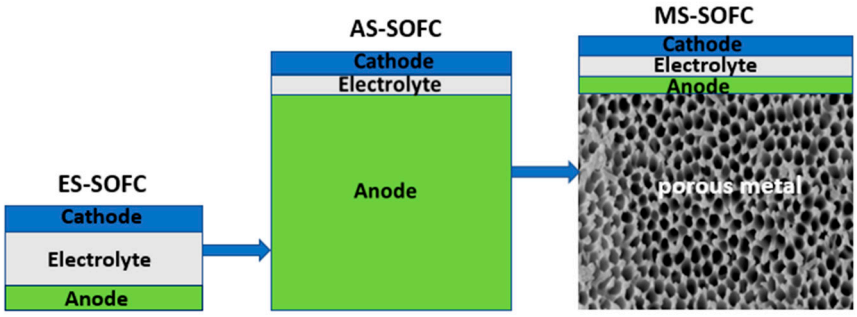

Figure 2. Different generations of SOFCs.

The addition of a thick support layer to traditional anode cells results in a stronger mechanical structure, as depicted in Figure 3. However, the layer is typically made of ceramic or cermet materials which are expensive, brittle, and susceptible to failure during the redox cycle. The conventional anode support is particularly vulnerable to thermal shock due to its brittle nature and can crack with rapid temperature cycling. Even Ni-YSZ-supported cells with their ceramic structure can fail during the redox cycle, even with slow heating [12,13].

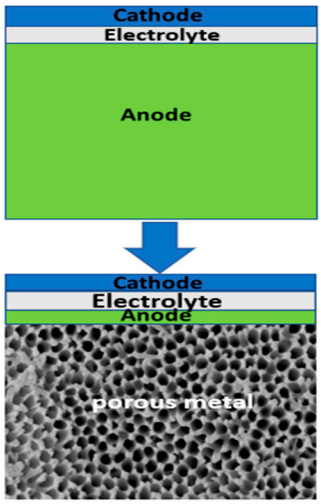

Figure 3. Schematic representation of the anode and metal support.

To avoid these problems, the use of metal supports is preferred, which is also less expensive, as shown in Figure 3 [11,14].

The carrier metal base is able to provide the fuel cell with greater mechanical strength compared to cells on a carrier electrode or electrolyte. In this regard, this design is attractive for applications in mobile autonomous power plants. The presence of a rigid support allows the remaining electrochemically active layers of the fuel cell (electrodes and electrolyte) to be formed in the form of thin films. However, in practice, the thickness of the functional elements of the fuel cell is determined by the method of their formation. This is also due to the necessity to maintain the efficiency of energy conversion since the energy conversion efficiency ε depends on the layer thickness L for the electrolyte with pronounced maximum depending on a current density [15,16].

In most cases, stainless steels are used for the manufacture of SOFC load-bearing metal bases [17], which is because they have a thermal expansion coefficient (TEC) close to other components of fuel cells and high resistance to oxidation [13,16,18].

Researchers at Lawrence Berkeley National Laboratory (LBNL) have developed metal-supported proton-conducting solid oxide fuel cell designs. The transportation of protons through electrolytes provides several benefits across different temperatures. For

instance, during electrolysis, the transport of protons generates pure hydrogen, thus eliminating the need to remove steam from the product stream. In fuel cell operation, extracting hydrogen from the anode through the electrolyte can accelerate fuel decomposition or reforming reactions. Additionally, proton ceramic fuel cells (PCFCs) exhibit resistance to carbon coking and sulfur, enabling stable operation with a broad range of hydrocarbon fuels [18–21].

MS-SOFCs are typically composed of three layers: an anode, an electrolyte, and a cathode. The electrolyte layer separates the anode and cathode and allows ions to move from one electrode to the other. The anode is where the fuel is oxidized, and the cathode is where oxygen is reduced [12,15,16].

There are three main types of MS-SOFC structures: planar, tubular, and flat-tubular. Planar MS-SOFCs. Planar MS-SOFCs have a flat, sandwich-like structure, where the anode, electrolyte, and cathode are stacked on top of each other. The electrolyte layer is typically made of a dense ceramic material, such as yttria-stabilized zirconia (YSZ). The anode is usually made of a porous metal such as nickel, and the cathode is made of a mixed conductor oxide, such as lanthanum strontium manganite (LSM) [14,16,22].

Advantages: 1. High power density due to the thin electrolyte layer. Simple manufacturing process due to the planar structure. 2. Low cost compared to other MS-SOFC structures [23].

Disadvantages: 1. Limited durability due to the thermal and mechanical stress during operation. 2. Difficult to seal and stack [16].

Tubular MS-SOFCs. Tubular MS-SOFCs have a cylindrical structure, where the electrolyte layer is coated on the inner surface of a tubular support. The anode and cathode are then coated on the outside and inside of the electrolyte layer, respectively.

Advantages: 1. High durability due to the tubular support structure. 2. Good mechanical stability due to the cylindrical shape. 3. High fuel utilization due to the long and thin tubular design.

Disadvantages: 1. Lower power density compared to planar MS-SOFCs. 2. Complex manufacturing process due to the tubular structure [16,24,25].

Flat-tubular MS-SOFCs. Flat-tubular MS-SOFCs are a combination of planar and tubular structures, where the electrolyte layer is coated on the inner surface of a flat tubular support. The anode and cathode are then coated on the outside and inside of the electrolyte layer, respectively. The flat-tubular support provides both mechanical and thermal stability to the cell.

Advantages: 1. High durability due to the flat-tubular support structure. 2. Good mechanical stability due to the cylindrical shape. 3. High power density due to the thin electrolyte layer.

Disadvantages: 1. Complex manufacturing process due to the flat-tubular structure. Difficult to seal and stack [26–28].

2. Materials of MS-SOFC

In the design of SOFC with a supporting metal base, the formation of layers of an electrochemically active cell occurs on the surface of a porous, and, as a rule, highly corrosion-resistant steel support. For this, various powder technologies are used, such as slip casting, screen printing, the sol-gel method, and others that require high-temperature sintering [13,26,29]. However, the application of these methods is associated with several difficulties; for example, the oxidation of the metal base during the sintering of the anode layer results in a significant decrease in electrical conductivity, which leads to a decrease in the efficiency of SOFC [19,24]. Therefore, a few stringent requirements are imposed on materials intended for the manufacture of metal bases. Firstly, such a material should have a TEC close to the TEC of other functional layers of the fuel cell to prevent the mechanical destruction of the cell during thermal cycling from room temperature to the operating temperature of SOFC. Secondly, the pore structure of the substrate material must provide free access of reagents to the working zone and removal of reaction

products from it, be resistant to a redox atmosphere, and have chemical stability at SOFC operating temperatures [14,22,29].

A typical SOFC consists of at least three components, and in the case of a metal-based solid oxide fuel cell, their number increases to four. These components work together to produce electrical current; thus, their compatibility with one another is important. The main candidates for employment in MS-SOFC as materials of its components are shown in Table 1.

Table 1. Candidate materials for MS-SOFC.

Cell	Materials	TEC (ppm/K)
Cathode	LSM, LNF, LSCF, SSC, LSC	12, 12, 18, 18.4, 22
Diffusion barrier layer	GDC	12.7
Electrolyte	YSZ, SCSZ, LSGM, GDC	10, 10.5, 12.7, 12.7
Anode	Ni/YSZ, Cu/YSZ, Titanates	12
Diffusion barrier layer	GDC	12.7
Metal support	Ni, Ni-Fe (1:1), Ferritic stainless steel	16.5, 13.7, 10–12

2.1. Substrate Materials

Over the years, scientists have experimented with various metals to be used as a substrate in MS-SOFCs. The selection process considers certain factors such as:

1. Compatibility with other materials used in SOFCs, particularly during heating and cooling phases.
2. High ability to resist oxidation.
3. High ability to withstand thermal cycling.
4. High electrical conductivity.
5. Low cost of materials [14,30].

Metal-supported SOFCs have been developed using substrates made from different metal compositions, such as Ni, FeNi, NiCrAlY, and ferritic stainless steel. Among these, FeCr-based ferritic stainless steels are commonly used due to their low cost, high resistance to oxidation at high temperatures, and similar thermal expansion to YSZ (a material commonly used in SOFCs), as discussed by Tucker et al. [19]. Ferritic stainless steel usually contains between 10.5 to 26 wt.% of Cr, and Al can be added to form a protective layer of Al_2O_3 on the surface of the steel, which helps to resist further oxidation [31].

In their research, Xia et al. [32] utilized SS-430L as the metal substrate in their MS-SOFCs, resulting in a peak power density of 246 MW/cm^{-2} at a temperature of 700 °C. However, there have been concerns raised regarding the suitability of SS-430L. For example, a previous investigation [33] revealed that the chromium content of 16–18% in SS-430L is inadequate for forming a protective coating against oxidation when employed as a base metal for SOFC deposition. Despite the conductivity of the chromium scale, it still represents the path with the least conductivity between the electrolyte and current collectors [24], which can slightly elevate the overall ohmic resistance of the circuit. Furthermore, prolonged oxidation can cause the SS-430L structure to fracture, leading to a disruption of electrical pathways [25]. Researchers have determined that once a chromium layer reaches a thickness of 5 µm, SS-430L is prone to splitting [26].

According to the findings of Tucker et al. [27], it was observed that the SS-430L MS (metal substrate) on the cathode side (air) developed a chromium scale measuring approximately 0.9 µm in thickness after 1200 h of operation. By extrapolating the growth rate of the scale, the researchers concluded that the cell could potentially function for up to 30,000 h before experiencing cleavage. However, another important aspect to consider when using ferritic stainless steel is the presence of silicon and aluminum, which have the potential to form non-conductive oxides during operation. A previous study has

highlighted that even a silicon content as low as 0.017 wt.% can undergo oxidation in stainless steel [34].

In addition to SS-430L, Fr-Cr alloys such as Crofer 22APU and 22H have been utilized as metal supports due to their higher chromium content, ranging from 20–24 wt.%, which offers improved resistance to oxidation. To compare their performance, the area resistivity of APUcrofer22 (0.02–0.03 Ω cm^2) was found to be lower than that of SS-430L (0.1 Ω cm^2) after exposure to air at 800 °C for 200 h [28], demonstrating its superior electrical conductivity [35]. Sarasqueta-Zabala et al. [36] conducted a study on the oxidation of Crofer 22APU in 50% humidified hydrogen at 800 °C. They observed that the growth of the chromium scale primarily occurs within the initial 500 h of operation, with only a slight increase in its thickness up to 4500 h. After 3000 h of operation, the dross thickness was measured at a mere 1.6 µm.

One notable drawback of these materials is the presence of chromium, which, due to prolonged operation of the fuel cell at SOFC operating temperatures (around 800 °C), can diffuse to the anode surface and form compounds such as Cr_2O_3. These compounds can lead to the degradation of the anode and adversely affect its electrochemical properties [29].

Stainless steels are commonly utilized as supportive metal substrates in SOFCs because they have a coefficient of thermal expansion (TEC) that closely matches other fuel cell components, and they exhibit high resistance to oxidation. However, a challenge arises at high temperatures where a reaction occurs between the iron (Fe) and chromium (Cr) present in the metal substrate and the nickel (Ni) in the anode. This reaction results in a decline in the catalytic activity of the anode [30]. To address this issue, diffusion barrier layers are applied between the metal base and the anode to prevent such interactions [37]. Another approach to circumvent the interaction of chromium with nickel is to fabricate metal substrates based on nickel (Ni) itself [38], or through the use of bimetallic compounds such as Ni-Fe [39] or Ni-Al [40]. These alternative materials help mitigate the adverse effects of chromium on the catalytic activity of the anode.

Solovyev et al. [41] fabricated and studied SOFCs on a Ni-Al carrier base with an electrolyte of yttrium-stabilized zirconia (YSZ). However, Ni-Al has a TEC (~15 $\times$ 10^{-6} K^{-1} at 800 °C [42]) that is much higher than the TEC of YSZ electrolyte (10.7–11 $\times$ 10^{-6} K^{-1} [43]). It is possible to reduce the TEC of Ni-Al by adding a substance with a low TEC to the composition of the material. In [44], the following ceramics were used as additives to Ni-Al: ZrO_2, ZrO_2-SiO_2, Al_2TiO_5, Al_2O_3, and an unspecified XO_2 oxide. It was shown that the addition of 35–40% inert oxide XO_2 reduces the TEC of the resulting composite to 12 $\times$ 10^{-6} K^{-1}.

2.2. Anode Materials

The primary role of the anode is to facilitate the electrochemical oxidation of fuel and to transport electrons to the external circuit. To fulfill these functions effectively, the anode material should possess certain characteristics. These include:

(1) High electrical conductivity: The anode material should exhibit a high level of electrical conductivity to facilitate efficient transportation of electrons from the active sites to the external circuit.
(2) High activity for fuel oxidation: The anode material should have a high level of activity towards the oxidation of fuel, enabling effective electrochemical reactions.
(3) Compatible thermal expansion coefficient (TEC): The anode material should have a TEC that is compatible with the electrolyte material. This is important to prevent warping or cracking of the fuel cell during start-up or cool-down processes [45,46].

According to reference [47], a material called $La_{0.4}Sr_{0.4}Fe_{0.03}Ni_{0.03}Ti_{0.94}O_3$ (LSFNT) was employed as the primary anode material in an MS-SOFC. The LSFNT backbone was infused with a Ni-GDC precursor solution, which was then thermally decomposed to form Ni-GDC. At a temperature of 700 °C, a maximum power density (MPD) of 0.77 W/cm^{-2} was achieved with a fuel utilization (FU) of 51%. The system's durability was tested for a

duration of 800 h, during which the power density degradation rate was determined to be 0.151 W/cm^{-2}·h.

The literature suggests that both yttria-stabilized zirconia (YSZ) and samarium-doped ceria (SDC) have the ability to stabilize nickel (Ni) in the anode and decrease anode polarization resistance. However, when Ni is combined with SDC, it demonstrates better performance compared to when Ni is mixed with YSZ [48,49].

Zhan Zh and his colleagues from the Shanghai Institute of Ceramics, Chinese Academy of Sciences, have developed a Nano-SDC@430L anode by infiltrating nano $Sm_{0.2}Ce_{0.8}O_{2-\delta}$ (SDC) into macro-porous 430L stainless steel scaffolds. This anode exhibited remarkable catalytic activity for hydrogen electro-oxidation, demonstrating low polarization resistances of 0.10 ± 0.01 and 0.18 ± 0.03 Ω cm^2 at temperatures of 800 and 700 °C, respectively. The outstanding redox properties of the anode, coupled with the high conductivity of the supporting 430L scaffolds, contribute to its exceptional performance. Fuel cells incorporating these anodes, combined with thin yttria-stabilized zirconia electrolytes, achieved promising power densities of 0.94 W/cm^{-2} at 800 °C and 0.55 W/cm^{-2} at 700 °C. This innovative structural design not only addresses the challenges in anode preparation for MS-SOFCs but also presents a new approach to fabricating high-activity anodes [50].

A group of researchers from the Shanghai Institute of Ceramics, Chinese Academy of Sciences, has made significant progress in developing nickel-free anode materials [51,52]. In their study, they utilized $Sr_2Fe_{1.5}Mo_{0.5}O_{6-d}$ (SFMO) as the anode material in a metal-supported solid oxide fuel cell (MS-SOFC). The SFMO-based anode exhibited an area specific resistance (ASR) of 0.11 $\Omega \cdot cm^2$ and a maximum power density of 0.81 W/cm^{-2} at 800 °C, with a 16 wt% anode loading.

A comparison was made between SFMO, $La_{0.6}Sr_{0.4}Fe_{0.9}Sc_{0.1}O_{3-d}$ (LSFSc) combined with yttria-stabilized zirconia (YSZ) and LSFSc combined with $La_{0.9}Sr_{0.1}Ga_{0.8}Mg_{0.2}O_{3-\delta}$ (LSGM) in terms of polarization resistance and maximum power density. At 800 °C, the polarization resistances were 0.11 $\Omega \cdot cm^2$ for SFMO, 0.21 $\Omega \cdot cm^2$ for (LSFSc) | YSZ, and 0.90 $\Omega \cdot cm^2$ for LSFSc | LSGM. The maximum power density exhibited an inverse trend to the ASR, with SFMO demonstrating the highest value.

The inferior performance of LSGM could be attributed to its lower ionic conductivity compared to YSZ. To enhance the performance of the LSFSc | LSGM system, copper was added, resulting in a reduction of the ASR to 0.58 $\Omega \cdot cm^2$ and an increase of the maximum power density from 0.18 to 0.54 W/cm^{-2}. In comparison to a nickel-samarium-doped ceria (Ni-SDC) anode, an ASR of 0.096 $\Omega \cdot cm^2$ was reported.

In the study referenced as [53], Persson et al. conducted an investigation into the performance of ruthenium and nickel in conjunction with GDC (gadolinium-doped ceria). The researchers discovered that ruthenium demonstrated superior electrochemical performance in comparison to nickel. More specifically, the fuel cells utilizing ruthenium exhibited a lower ASR of 0.322 $\Omega \cdot cm^2$, whereas the cells utilizing nickel displayed a higher ASR of 0.453 $\Omega \cdot cm^2$. Additionally, the limiting current density was higher for the cells incorporating ruthenium compared to those using nickel.

Interlayer diffusion of nickel (Ni) and chromium (Cr) poses a significant challenge when employing a nickel-based anode electrocatalyst in MS-SOFC with the MS configuration on the anode side [54,55]. The migration of chromium into the anode layer has the potential to generate chromium oxide scales on active sites, thereby elevating the anode's polarization resistance [56]. In a similar vein, the diffusion of nickel into steel can induce alterations in the microstructure of the steel material, leading to the conversion of ferritic stainless steel to austenite due to its reaction with nickel.

Anode materials in MS-SOFCs play a crucial role in the electrochemical performance of the fuel cell. In addition to polarization resistance, other important factors that influence anode performance include:

1. Electrochemical activity: The anode material must be electrochemically active to catalyze the oxidation of the fuel. This activity is usually evaluated by measuring

the anode's electrochemical oxidation current density and comparing it with the theoretical current density calculated from the fuel's chemical reaction kinetics.

2. Gas transport: The anode material should have good gas transport properties to ensure efficient fuel supply and exhaust. This is particularly important for high-performance MS-SOFCs where the anode material should allow for rapid transport of fuel and waste gases while minimizing mass transport losses and reducing the likelihood of fuel starvation.
3. Chemical stability: The anode material should have good chemical stability, meaning that it should not undergo any chemical reactions that could lead to its degradation or failure over time. This is particularly important in MS-SOFCs, where the anode is often exposed to harsh chemical and thermal environments.
4. Microstructure: The anode material should have a well-defined microstructure with good porosity and tortuosity. This allows for efficient fuel distribution and diffusion while minimizing mass transport losses and ensuring high electrochemical activity.
5. Adhesion to metal support: In MS-SOFCs, the anode material is deposited onto a metallic support. The anode material should have good adhesion to the metal support to prevent delamination and ensure mechanical stability during cell operation.
6. Redox stability: The anode material should have good redox stability, meaning that it should be able to tolerate repeated changes in oxidation state without undergoing any significant changes in its microstructure or electrochemical activity. This is particularly important for MS-SOFCs that operate under cyclic or transient conditions [45].

As an anode material, Ni has been widely used in SOFCs due to its high electrochemical activity towards hydrogen oxidation, which is the most commonly used fuel in SOFCs. Ni-based anodes can also be easily fabricated using cost-effective methods such as screen printing or spray coating, making them attractive for large-scale production [57].

As a metal support material, Ni has several advantages, such as its high thermal conductivity, low coefficient of thermal expansion, and compatibility with high-temperature SOFC operating conditions [58]. Ni-based metal supports can also be easily processed and have been shown to provide excellent mechanical stability and resistance to thermal shock [59,60].

By combining the functions of anode and metal support into a single Ni-based layer, MS-SOFCs can offer several advantages over traditional SOFC designs. For example, the use of a Ni-based anode/metal support layer can lead to a reduction in cell thickness, which can improve the fuel cell's performance and reduce manufacturing costs. Moreover, the integration of anode and metal support functions can simplify the fuel cell's design, leading to improved reliability and durability [46,52].

The reason for this is that it is the most active catalyst for electrochemical oxidation and that the aforementioned problems can be solved by making structural changes to MS-SOFC [61], such as adding thin layers of a micron-level diffusion barrier [51,62,63].

2.3. Electrolyte Materials

The electrolyte plays a crucial role in the functioning of the SOFC, as it carries negative oxygen ions and completes the electrical circuit while also providing oxygen ions for the reaction with the fuel at the anode. To ensure optimal performance, the micro- and macrostructure of the electrolyte must meet several key requirements [46,64,65].

Firstly, the electrolyte body must be dense to minimize the chance of fuel or oxidizing gas diffusing to the other side and causing reactants to react without forming an external current. This also ensures good ionic conductivity by providing a cohesive path for the transport of oxygen ions [66]. Secondly, the electrolyte must adhere to the anode and cathode layers to avoid delamination of layers and cracks between layers, which can lead to cell failure. Lastly, electrolyte shrinkage during manufacturing must correspond to the shrinkage of all components to avoid any issues [67,68].

To meet these requirements, most electrolytic materials are doped zirconium or cerium oxides [69,70]. The crystal structure of these oxides contains oxygen positions that are fixed,

forming a pathway for oxygen within the material. Introducing a low-valent cation as a dopant in the oxide creates oxygen vacancies, which serve as pathways for oxygen ions. According to existing literature, dense electrolytes typically exhibit an open circuit voltage (OCV) slightly above 1V when hydrogen is used as the fuel source [46].

Protonic electrolytes have several advantages over oxide-ion conductors in MS-SOFCs. They have higher proton conductivity at lower temperatures, which makes them suitable for use in MS-SOFCs that operate at lower temperatures than traditional SOFCs. The main characteristics of protonic electrolytes for MS-SOFC and their sealing methods are presented in Table 2 [71].

Table 2. Main characteristics of protonic electrolytes for MS-SOFC and their sealing methods.

Electrolyte Material	Electrolyte Thickness	OCV, Temperature	Polarization Resistance	Maximum Power Density, Temperature	Sealing Method	Ref.
$BaZrO_3$-based electrolytes	30–50 µm	1.1 V at 500 °C	0.4 Ω cm^2	66 mW/cm^2 at 550 °C	Ag paste	[72]
$SrZrO_3$-based electrolytes	10–30 µm	1.0 V at 450 °C	0.3 Ω cm^2	300 mW/cm^2 at 700 °C	glass-ceramic sealant	[73]
H_3PO_4-doped SrZrO3-based electrolytes	10–30 µm	0.9 V at 400 °C	0.1 Ω cm^2	17 mW/cm^2 at 500 °C	glass-ceramic sealant	[74]
Nafion-based electrolytes	5–10 µm	0.4 V at room temperature	0.5 Ω cm^2	2 mW/cm^2 at 80 °C	glass-ceramic sealant	[75]

To achieve the maximum densification of the electrolyte, high sintering temperatures are necessary. However, this process may cause deformation and alterations in the microstructure of the metal substrate and anode [67].

When it comes to MS-SOFCs, many designers show a preference for utilizing YSZ (yttria-stabilized zirconia) as the electrolyte material due to its numerous advantages compared to other electrolyte materials. YSZ offers notable stability, well-defined cost, and exceptional performance [76]. Furthermore, the YSZ electrolyte exhibits pure ionic conductivity and remarkable stability, enabling the operation of SOFCs at high temperatures exceeding 650 °C. In contrast, the CGO (cerium gadolinium oxide) electrolyte demonstrates significant electronic conductivity at temperatures above 600 °C [77]. The high operating temperature capability of YSZ electrolyte facilitates the internal reforming of hydrocarbon fuels, eliminating the need for an external pre-reformer [48].

A significant challenge related to the utilization of YSZ electrolyte is the inability to achieve full density when working with limited geometries. In order to tackle this issue, scientists have explored various methods [78]. These include the deposition of a dense layer of YSZ using techniques such as plasma or flame spraying, as well as co-sintering with a wet substrate after the colloidal/wet deposition of YSZ to achieve full density [49].

The future discussion will delve into the advantages and disadvantages of the methods used to create a dense electrolyte on a metal surface. One approach involves utilizing YSZ plasma spraying to deposit a nearly dense layer of YSZ onto an existing metal substrate. The subsequent full densification is achieved through heat treatment at a relatively lower temperature, which helps maintain the high porosity of the metal substrate during fabrication. However, in order to ensure gas-tightness, the electrolyte layer must have a thickness ranging from 30–70 µm. Moreover, several sources have observed that the apparent ionic conductivity of plasma-deposited YSZ is lower compared to sintered YSZ [79,80].

The co-sintering technique encompasses the application of a slender and permeable layer of YSZ onto a metal substrate in its initial state, employing wet/colloidal deposition methods such as tape flooding, drip coating, screen printing, spray coating, dip coating, and spin coating. Subsequently, the green layers are subjected to high-temperature sintering from 1200–1400 °C to achieve a compact electrolyte structure. This method presents a

favorable advantage for large-scale industrial production due to its cost-effectiveness in manufacturing [43,47].

In contrast to plasma spraying, wet/colloidal deposition methods offer the capability to deposit and sinter a thin YSZ layer (10–20 μm). This allows the cell to function within a relatively lower temperature range (650–700 °C), which helps prevent rapid oxidation of commonly utilized stainless steel substrates. During the sintering process, YSZ undergoes shrinkage of 10–25% based on the green density. It is crucial to ensure that the substrate's shrinkage matches that of the electrolyte to avoid tension-induced cracks during co-sintering. Achieving the appropriate level of warp shrinkage while maintaining sufficient porosity can be challenging, but it is achievable through a meticulous combination of factors such as particle size, granulometry, initial packing density, blowing agent quantity, and binder count [49,81].

Co-sintered MS-SOFCs have demonstrated remarkable performance, stability, thermal cycling resistance, and redox cycling resistance according to reports [55]. Additionally, alternative electrolyte materials such as Sc_2O_3-ZrO_2 [82], Bi_2O_3-doped cerium oxide [83], and lanthanum strontium magnesium gallate perovskite (LSGM) are being explored due to their enhanced ionic conductivity [64]. Scandium-doped zirconia exhibits similar properties to yttria-zirconium oxide, with a 9% Sc_2O_3-ZrO_3 composition showcasing nearly twice the ionic conductivity of 8YSZ at 1000 °C [84]. However, the limited availability and high cost of Sc_2O_3 make it unfeasible for large-scale applications of SOFCs [81,85].

Apart from Sc_2O_3-ZrO_2, other families of electrolytes such as doped cerium oxide and doped Bi_2O_3 exhibit electronic conductivity above 600 °C, necessitating the application of a thin YSZ layer for protection [86]. The ionic conductivity of gadolinium-doped cerium oxide electrolyte (CGO-$Ce_{0.9}Gd_{0.1}O_{1.95}$) at 600 °C is equivalent to that of YSZ at 800 °C. However, the reduction of Ce^{4+} ions to Ce^{3+} in CGO can lead to electron short-circuiting caused by electronic conduction and undesired lattice expansion [65]. It has been observed that SOFCs with CGO electrolytes can operate at lower temperatures, approximately 500 °C, where the influence of electronic conductivity is insignificant. Furthermore, low-temperature ferrite supports components and sealing materials utilized within this temperature range [65].

2.4. Cathode Materials

The cathode plays a crucial role in the process of reducing oxygen to oxygen ions in solid oxide fuel cells (SOFCs). Typically, cathodes are composed of doped metal oxides that provide active sites for oxygen adsorption and reduction. Various cathode materials, including LSCF, LSC, LSM, and SBSCo, have been evaluated and classified based on their polarization and reactivity with the electrolyte [87]. The cathode is commonly applied in the form of a suspension, which is subsequently dried and sintered to ensure proper adhesion to the electrolyte. However, this cathodic sintering method can give rise to challenges such as high cathode polarization or catalyst inactivity due to changes in the crystal structure of the doped metal oxides at elevated sintering temperatures in a reducing atmosphere. In the case of metal-supported solid oxide fuel cells (MS-SOFCs), YSZ is a frequently used electrolyte material due to its ease of handling. However, many commercial cathode materials react with YSZ, leading to physical alterations in the electrolyte and cathode layers, ultimately reducing the lifespan of the cell [62,87,88].

Selecting a cathode for sintered cells is a complex process that requires consideration of several factors. To prevent oxidation of the metal carrier during sintering operations, a reducing atmosphere is typically used. Cells on a metal support also require processing in an inert or vacuum atmosphere, which can cause standard cathode catalysts to decompose [68]. Therefore, cathodes are usually deposited on metal supports after completion of all processing steps in a non-oxidizing atmosphere [89]. While cathodes are usually processed in air, the maximum sintering temperature must be kept below approximately 900 °C to avoid oxidation of the metal base [90]. This restriction limits the choice of cathode since conventional compositions such as LSM (LaMnO3 doped with Sr) and LSCF (lan-

thanum cobaltite strontium ferrite) require sintering in air in the range of 1000–1200 °C to achieve high performance [48,91,92].

High-temperature solid oxide fuel cells (SOFCs) often use a cathode material called strontium-doped lanthanum manganite ($La_{1-x}Sr_xMnO_3$ or LSM) from the perovskite manganite family, where strontium partially replaces lanthanum [93]. Perovskite structures can have different compositions and oxygen levels, which affect their electrical and catalytic properties. This cathode material performs better at high temperatures, particularly above 800 °C [94], but if there is too much lanthanum or strontium oxide, it can form an insulating phase (such as $La_2Zr_2O_7$ or $SrZrO_3$) when it interacts with zirconium oxide (a stabilizer), leading to poor performance [95].

To address this issue, one solution is to increase the concentration of manganese while keeping the fabrication temperature below 1300 °C. At 900 °C, strontium-doped lanthanum manganite (LSM) has low oxygen ion conductivity but high electrical conductivity [96]. As a result, the reaction area is limited to the interface between the electrode and electrolyte. To enable oxygen reduction, the cathode must be sufficiently porous to allow oxygen diffusion at this interface. In practice, a composite layer or a gradient LSM/YSZ structure can increase the number of triple-phase boundaries [88].

The process of cathodic reaction in materials with electronic conductivity, such as perovskites, can occur through different stages and mechanisms depending on the type of electrode material. The surface path is the most appropriate mechanism for the cathodic reaction in intact electronic conductors [62]. In mixed ion-electronic conductors, the common path is the typical mechanism, while in composite materials such as LSM/YSZ, the electrolyte surface path is considered. Figure 4 illustrates three different pathways for oxygen reduction [87].

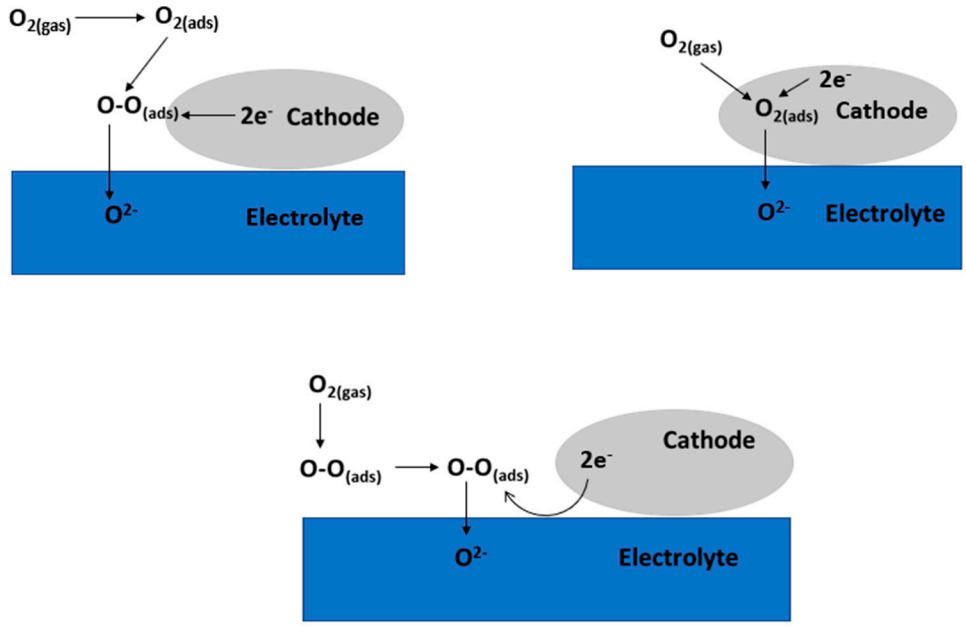

Figure 4. Three ways of oxygen reduction reaction.

There is a significant focus on enhancing the efficiency of electrodes for low- and medium-temperature solid oxide fuel cells (SOFCs) [67]. Researchers have explored various cathode materials with improved electronic/ionic conductivity and higher oxygen exchange rates, which can extend the oxygen reduction process within the cathode structure or at the fuel/cathode junction, thereby increasing the reaction rate. To this end, other perovskite materials such as $La_{1-x}Sr_xFe_{1-y}Co_yO_3$ (LSCF) are being studied [68]. In a research study [97], LSM-YSZ (composite) and LSCF cathodes with YSZ-CGO electrolyte were investigated using current-over-potential measurements and impedance spectroscopy. The

findings revealed that at an operating temperature of 850 °C, LSM-YSZ exhibited a higher polarization resistivity of 1.8 $\Omega \cdot cm^2$, whereas LSCF demonstrated a lower polarization resistivity of 0.4 $\Omega \cdot cm^2$ [98,99].

Blennow et al. [100] conducted a study to investigate the use of a GDC diffusion barrier layer between YSZ and cathode catalysts containing cobalt and strontium (LSCF and LSM). Two methods of applying the barrier layer were evaluated: physical vapor deposition (PVD) and spinning. The results indicated that a dense barrier layer deposited with PVD was effective in blocking the reaction between LSCF and LSM.

Franco et al. [48] conducted a study on the utilization of a thin magnetron sputtered GDC (gadolinium-doped ceria) barrier layer in combination with LSF, LSCF, and LSM cathodes. They investigated the performance of these cathodes with different cobalt contents in $La_{0.8}Sr_{0.2}Co_{1-x}Mn_xO_{3-\delta}$ (LSCM) through their study [101]. The findings indicated that a cobalt content of 40% resulted in optimal performance. Higher cobalt content can lead to reactions with the YSZ electrolyte, and cobalt content exceeding 40% in LSCM can cause a change in its thermal expansion coefficient (TEC), leading to cracking. To address this issue, Bae et al. explored the use of chromium-containing cathodes, varying the chromium content in $La_{0.8}Sr_{0.2}Cr_{1-x}Mn_xO_{3-\delta}$ (LSCrM) from 0 to 80%. They also investigated a binary cathode composed of LSCrM and 5% ruthenium [102].

The researchers reported that replacing cobalt with chromium enabled the cathode to be sintered in an inert atmosphere. It is worth noting that the selection of cathode materials extends beyond the compounds mentioned above, and there is ongoing active research and exploration for effective cathode materials in the field.

3. Degradation Processes in MS-SOFC Electrodes

The high operating temperatures (600–1000 °C) of solid oxide fuel cells (SOFCs) make all of their components susceptible to degradation, resulting in a decline in the power output of metal-supported solid oxide fuel cells (MS-SOFCs) [92]. This degradation occurs as the functional properties of the components deteriorate over time. Degradation phenomena are difficult to classify because are a combination of physicochemical processes of various natures, for example, the sintering of electrode particles [103], the effect of electrode polarization [104], and the poisoning effect of a gas environment, in many cases, occurring in parallel [105]. However, it should be noted that the depth (degree) of degradation can be determined both by a combination of many phenomena and only by one dominant process [106–108].

3.1. Carbon Deposition Problems

Carbon deposition occurs when hydrocarbons in the fuel stream are not fully oxidized at the anode surface and instead deposit carbon on the anode material. Carbon deposition can lead to several degradation mechanisms in MS-SOFCs, including:

- Reduced electrochemical activity: Carbon deposited on the anode surface can block the active sites and reduce the effective surface area available for electrochemical reactions, leading to decreased anode activity and cell performance.
- Increased polarization resistance: Carbon deposition can increase the polarization resistance of the anode, making it more difficult for electrons to be transferred from the anode to the cathode, resulting in decreased cell performance.
- Formation of carbonates: Carbon deposition can also lead to the formation of carbonates on the anode surface, which can further reduce the electrochemical activity and lead to reduced cell performance [102].
- Several factors can contribute to carbon deposition in MS-SOFCs, including the fuel composition, operating temperature, and anode material properties. Strategies to mitigate carbon deposition in MS-SOFCs include:
- Increasing the operating temperature: Raising the operating temperature can promote more complete oxidation of hydrocarbons at the anode surface and reduce the likelihood of carbon deposition.

- Use of reforming catalysts: Catalysts can be used to promote more complete oxidation of hydrocarbons and reduce carbon deposition on the anode surface.
- Optimization of fuel composition: The fuel composition can be optimized to reduce the concentration of hydrocarbons and other species that are prone to carbon deposition.
- Anode design: The anode design can be optimized to promote a more uniform distribution of fuel and oxygen and reduce the likelihood of hot spots that can promote carbon deposition [91].

Carbon deposition is a significant degradation mechanism in MS-SOFCs that can lead to reduced cell performance and efficiency. Strategies to mitigate carbon deposition can help improve the long-term stability and performance of MS-SOFCs [109].

3.2. Anode Problems

Ni-YSZ composites are commonly used as the main material for SOFC anodes and also serve as the carrier base of the fuel cell. The ceramic component plays a crucial role in stabilizing the microstructure and preventing nickel particles from sintering while also expanding the zone of the electrochemical reaction at the interface between the three phases of electronic conductor/ionic conductor/gas. In addition, the tortuosity of the pores and the connectivity of individual phases are also important microstructural characteristics of nickel-ceramic anodes, which determine the stability of their functional characteristics over time [91].

The primary issue with using a nickel-based electrocatalyst in MS-SOFC (MS on the anode side) is the diffusion of nickel and chromium between layers [109]. Chromium can move into the anode layer and form deposits on active sites, which increases the anode's resistance to electrical current [110]. Similarly, nickel can diffuse into steel and alter its microstructure, causing ferritic stainless steel to become austenitic. To address this problem, one solution is to modify the structure of MS-SOFC by adding thin diffusion barrier layers (DBLs) at the micron level [100,111].

In their research, Kim et al. [54] developed innovative fuel cell half-cells. These half-cells consisted of a dense YSZ layer, a porous Ni-YSZ anode layer, and a stainless-steel (STS) ferrite substrate. Additionally, a layer of YST-CeO_2 composite material (approximately 60 mm thick) was incorporated into certain cells. This composite layer effectively prevented the diffusion of Fe and Ni while capturing evaporated Cr during the fabrication process conducted at high temperatures (1350 °C). When combined with a $La_{0.6}Sr_{0.4}Co_{0.2}Fe_{0.8}O_{3-d}$ (LSCF) cathode, the cell with the DBL configuration achieved an impressive maximum power density of approximately 220 MW/cm^2, which remained stable even at 700 °C.

3.3. Agglomeration and Enlargement of Nickel Particles

The degradation of Ni-YSZ anodes primarily occurs due to the agglomeration and growth of nickel particles. However, comprehensive studies on these phenomena have been limited due to their time-consuming nature. Only a handful of publications [112–114] have reported findings from such experiments. Symbolis et al. [112] demonstrated that the enlargement of nickel grains in nickel-ceramic anodes leads to various negative effects, including a reduction in the specific surface area of the anode, a decrease in the number of electrochemically active sites for fuel electrooxidation on the anode, and a decline in the level of percolation between nickel particles. Matsui et al. [115] observed that the degradation of nickel-ceramic anodes is accompanied by an increase in their ohmic resistance. The article demonstrates the relationship between changes in electrical conductivity and the particle size of the anodes. Additionally, Tanasini and Faes et al. [116] established a correlation between anode degradation, nickel particle growth, and a decrease in the length of the three-phase boundary (TPB) (Figure 5).

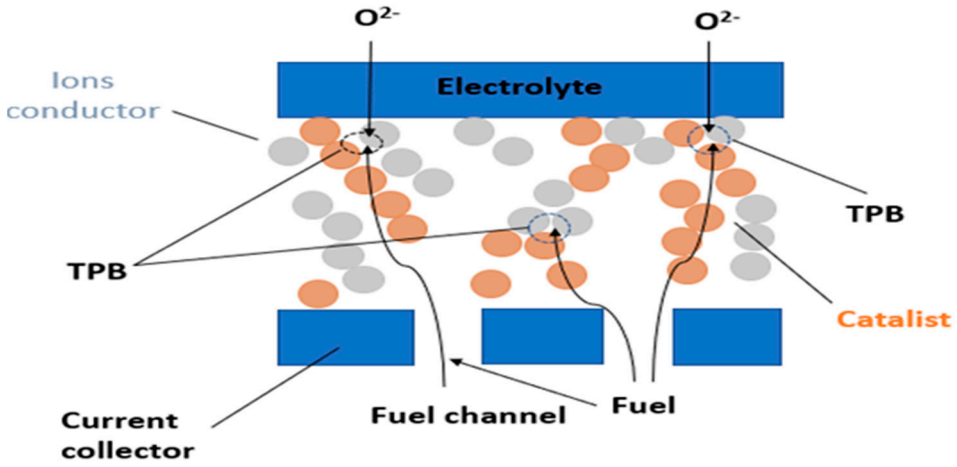

Figure 5. Schematic representation of the TPB.

Numerous studies have investigated the changes in resistance of anodes over time. It has been noted that the dependence of such changes has an exponential nature, and the time constant reflects the rate of degradation processes [107,108]. In their research, Pihlatie et al. [117] discovered that the electrical conductivity of Ni-YSZ anodes decreases over time and is influenced by external factors such as temperature and water content in the gas phase [118]. The study [107,108,115,116] described the time-dependent behavior of conductivity using a linear combination of two exponential functions with distinct time constants. This observation suggests the presence of two degradation processes occurring concurrently.

4. Cathode Problems

Conventional cathode materials such as LSM and $La_{1-x}Sr_xFeO_{3-d}$ (LSF) require sintering in an air atmosphere at temperatures ranging from 1000 to 1200 °C to ensure good adhesion with the electrolyte and acceptable electrochemical performance. However, such high temperatures can lead to excessive oxidation of the stainless steel substrate. To overcome this issue, a reducing atmosphere can be employed to protect the steel substrate, although it may result in the decomposition of these cathode materials. Alternatively, physical deposition techniques such as plasma spray can be utilized to avoid this problem [115]. However, due to the high cost associated with these deposition techniques, many researchers opt for the in-situ sintering method, which involves sintering the cathode during the cell testing process to fabricate cathodes for MS-SOFCs [116]. Kim et al. investigated the in-situ sintered $Ba_{0.5}Sr_{0.5}Co_{0.8}Fe_{0.2}O_{3-d}$ (BSCF) cathode and demonstrated good sinterability [119]. Nonetheless, the poor chemical compatibility between these in-situ sintered cathodes and zirconia-based electrolytes can reduce the overall stability of the fuel cells. Similar to the anode, cathode-related issues can be addressed by utilizing the infiltration method. The application of LSM-infiltrated YSZ cathode in MS-SOFCs has shown promising performance in the temperature range of 650–750 °C [27,108].

One of the primary issues with MS-SOFC cathode materials is the co-sintering process. To solve this problem, the sintering temperature of the cathode material can be lowered, or a cathode material that can be sintered in a reducing atmosphere at high temperatures can be used [117]. In a recent study [119], the authors suggested using a barium-containing cathode that can be sintered at lower temperatures (below 1000 °C). Substituting barium in the crystal structure can increase the interface resistance associated with the caking ability of the cathode particles and adhesion between the cathode and the electrolyte. In situ, the use of SBSCO50 and BSCF as cathodes resulted in very low ASR values of 0.020 $\Omega \cdot cm^2$ and 0.054 $\Omega \cdot cm^2$ at 800 °C operating conditions. Metal-supported cells with SBSC50 and BSCF cathodes at an operating temperature of 800 °C showed maximum power densities of 0.50 W/cm^2 and 0.65 W/cm^2, respectively.

When electrodes that have been impregnated are utilized, it allows for a wider range of cathode catalytic materials to be used. This is because catalytic materials with a high TEC (thermal expansion coefficient) can penetrate into the porous cathode base as nanoparticles [119–121], which avoids a mismatch between the cathode and the electrolyte. Additionally, the coarsening of the cathode microstructure caused by sintering can be avoided [122], as there is no need for additional sintering of the impregnated nanoparticles [109,123].

5. Problems with the Metal Support

The most commonly used materials for metal substrates are Crofer22APU steel, as well as a small number of special iron-chromium steels obtained by traditional metallurgical methods of sintering metal powders [124]. A significant disadvantage of such materials is the presence of chromium in them [125], which, because of the long-term operation of the fuel cell at SOFC operating temperatures (about 800 °C) [126], is able to diffuse to the anode surface with the formation of compounds of the Cr_2O_3 type [127], which destroy the anode and worsen its electrochemical characteristics [30,128,129].

To prevent this unwanted diffusion, barrier layers [130] are formed on the surface of porous metal plates [78,131]. The task of such a barrier layer is to prevent mutual diffusion of the materials of the metal substrate and the anode layer. In addition, the barrier layer should be electrically conductive and should not impede the gas flow, should be close to the rest of the layers of the TEC fuel cell, and should also be mechanically and chemically resistant to SOFC operating conditions. Spinels [132–134] or such composites as $La_{0.6}Sr_{0.2}Ca_{0.2}CrO_3$ [78], CeO_2, and $Ce_{0.8}Gd_{0.2}O_2$ [131] are used as efficient diffusion barrier layers.

Most of the chromium steels used have a TEC greater than that of ZrO_2:Y_2O_3 (YSZ), $Ce_{0.9}Gd_{0.1}O_{3-\delta}$ (CGO) or $La_{0.80}Sr_{0.20}Ga_{0.80}Mg_{0.20}O_{3-x}$ (LSGM) (10–12 ppm K^{-1}) electrolyte. The problem can be solved, as shown in the study [29], by introducing various additives into the composition of the main initial alloy. Thus, for example, the TEC of the initial Fe30Cr alloy was as close as possible to the TEC of the 8YSZ electrolyte by adding 3 wt.% $Al_{1.57}Fe_{0.43}TiO_5$ (AFT). A single cell with a Fe30Cr3AT base, a Ni/YSZ anode, a YSZ electrolyte 10–30 μm thick, and an LSM cathode at a temperature of 900 °C showed a maximum power density of 350 MW/cm^2 [29]. Data on the stability of such a cell during its long-term operation are not given in the article [29].

The bearing metal base is known to be made of pure nickel. However, this approach proved to be insufficiently effective due to the high cost of nickel, its significantly different TEC (16.5 ppm K^{-1}), and its low resistance to redox environment [135].

The addition of iron to nickel, as shown in [136,137], reduces the cost of the material, and equalizes the discrepancy between the TEC of pure nickel, but at the same time, the resistance to the redox atmosphere and to the effects of sulfur and to the coking of such materials remains quite low. With a ratio of Ni to Fe equal to 1:1, the TEC of the Ni-Fe system is 13.7 ppm K^{-1}, which is closest to the TEC of electrolyte materials. At the same time, the maximum performance was obtained by adding only 10 wt to nickel. % iron.

Excellent resistance to oxidation at operating temperatures up to 900 °C was demonstrated by the porous NiCrAlY alloy obtained by hot stamping and tested as the SOFC metal base [25]. However, the question arises about the mechanical stability of a fuel cell with such a metal base, since the TEC of NiCrAlY is 15–16 ppm K^{-1}, which significantly exceeds the TEC of the anode and electrolyte.

An alternative to the traditionally used chromium stainless steels, according to the project implementers, can be intermetallic alloys based on nickel and aluminum. Such compounds have better resistance to oxidation at high temperatures [138]. While significant research has been conducted on the oxidation resistance of bulk Ni-Al alloys and coatings [139,140], there is relatively limited published literature available regarding porous Ni-Al alloys. Furthermore, only a few studies have specifically focused on fuel cells based on porous Ni-Al alloys [141].

6. Sealing Problems of MS-SOFC

Sealing is a critical issue in MS-SOFCs, as it is essential to prevent gas leaks and maintain a stable operating environment. There are several sealing problems associated with MS-SOFCs, including:

1. Thermal expansion mismatch: The metal substrate and the ceramic components of the fuel cell have different coefficients of thermal expansion, which can cause stress and cracking at the interface between the two materials. This can lead to gas leaks and reduced performance.
2. Oxidation and corrosion: The high operating temperatures of MS-SOFCs can cause the oxidation and corrosion of the cell components, including the sealing materials. This can lead to gas leaks and reduced performance over time.
3. Sealant compatibility: The sealing materials used in MS-SOFCs must be compatible with both the metal substrate and the ceramic components of the fuel cell. If the sealant is not compatible, it can degrade and fail, leading to gas leaks and reduced performance.
4. Mechanical stability: The sealing materials must also provide mechanical stability to the cell components and maintain a tight seal under varying operating conditions. This requires careful design and testing of the sealing materials and assembly methods [142,143].

To address these sealing problems, researchers are exploring new sealing materials and designs that can better withstand the harsh operating conditions of MS-SOFCs. These include advanced ceramics, metal alloys, and composite materials that can provide improved thermal stability, corrosion resistance, and mechanical strength. Additionally, advanced manufacturing techniques, such as laser welding and plasma spraying, are being investigated to improve the precision and reliability of the sealing process [144].

For example, Sudireddy and colleagues utilized laser welding to seal an MSCs stack, which demonstrated a degradation rate of 0.5–1.2% per 100 h (over 2000 h) at 700 °C in moist hydrogen [145]. In 2019, Leah and her team at Ceres Power reported a better outcome, with the development of 1 kW stacks exhibiting a degradation rate of 0.2% per 1000 h (over 17,600 h) at 610 °C in reforming gas. This finding further promotes the full commercialization of MSCs [146].

Reference [147] explores the application of brazing technology to create a novel self-sealing structure for metal-supported solid oxide fuel cells (MS-SOFCs). This innovative design effectively addresses the sealing challenges on the anode side of planar SOFCs and achieves a highly reliable self-sealing effect. The cell's functional layers, including the anode, cathode, and electrolyte, are fabricated using plasma spraying technology. A single cell is assembled with a Sc_2O_3-stabilized ZrO_2 (ScSZ) electrolyte layer, which has a thickness of 50–60 μm, and the gas permeability of the self-sealed MS-SOFC without a cathode layer is measured at 0.42×10^{-17} m^2. The cell demonstrates an open-circuit voltage of approximately 1.1V within an operating temperature range of 550 to 750 °C. In standard atmospheric conditions, the cell achieves a power density of 1109 mW/cm^{-2} at 750 °C. Moreover, when the fuel gas pressure exceeds the cathodic gas pressure by 20 kPa, the cell's power density significantly increases to 1782 mW/cm^{-2} at 750 °C. The innovative cell structure, combined with the gas tightness of the ScSZ electrolyte produced through plasma spraying, indicates its suitability for SOFC applications.

7. Future Perspectives and Problems

MS-SOFCs have shown promising potential for efficient and clean energy conversion. However, there are still some challenges that need to be addressed before widespread commercialization can occur. Below, we will discuss in detail the future perspectives and problems of MS-SOFCs.

7.1. Future Perspectives

Despite the challenges, MS-SOFCs have great potential for a wide range of applications, including stationary power generation, transportation, and portable power devices. The following are some of the future perspectives of MS-SOFCs:

1. Enhanced Electrode and Electrolyte Stability: The development of new materials for the electrode and electrolyte layers is essential to improve the stability of MS-SOFCs. Research is currently focused on developing new cathode materials with improved catalytic activity and stability under high-temperature and corrosive conditions. Additionally, new electrolyte materials with higher ionic conductivity and improved chemical stability are being developed.
2. Low-Cost Substrates: The use of low-cost metal substrates such as iron and steel can significantly reduce the cost of MS-SOFCs. Research is ongoing to optimize the manufacturing process of MS-SOFCs and reduce the cost of the metal substrates.
3. Integration with Renewable Energy Sources: MS-SOFCs can be integrated with renewable energy sources such as solar and wind power to provide a reliable and sustainable source of electricity. This technology has the potential to revolutionize the energy sector by providing clean and affordable energy to remote and off-grid areas.
4. Miniaturization: MS-SOFCs can be miniaturized to create portable power devices for various applications such as laptops, mobile phones, and medical devices. The miniaturization of MS-SOFCs requires the development of new materials and manufacturing processes.

7.2. Future Problems

One of the major challenges is the high operating temperature required for MS-SOFCs, typically above 600 °C. This limits their use in certain applications, such as portable power sources. Lowering the operating temperature while maintaining high performance is therefore an important research direction for MS-SOFCs. Research efforts have been focused on developing new materials and device designs that can operate at lower temperatures without compromising performance.

Another challenge is the compatibility between the metal substrate and the ceramic layers. The high-temperature processing required for fabricating the ceramic layers can cause interdiffusion and reactions between the metal and the ceramics, which can degrade the performance and stability of the cell. Various strategies have been proposed to mitigate this issue, such as using a buffer layer or a ceramic interlayer to prevent direct contact between the metal and the ceramic layers. However, more research is needed to develop reliable and cost-effective strategies for addressing this issue.

The mechanical properties of the metal substrate can also affect the performance and stability of MS-SOFCs. The mismatch in the coefficient of thermal expansion between the metal and the ceramics can cause thermal stresses, which can lead to cracking and delamination of the cell. Developing metal substrates with improved mechanical properties, such as lower thermal expansion coefficient and higher strength, is, therefore, an important research direction. Additionally, advanced manufacturing techniques, such as additive manufacturing or roll-to-roll processing, can be used to fabricate metal-supported SOFCs with improved mechanical properties.

The cost of MS-SOFCs is another challenge that needs to be addressed. While metal substrates are generally less expensive than ceramic substrates, the cost of other materials, such as the ceramic electrolyte and the catalysts, can still be a barrier to the widespread adoption of MS-SOFCs. Research efforts have been focused on developing low-cost materials and fabrication techniques to reduce the overall cost of MS-SOFCs.

In terms of future perspectives, MS-SOFCs have the potential to be used in a wide range of applications, including stationary power generation, distributed power generation, and transportation. For example, MS-SOFCs can be used in hybrid vehicles, where they can provide power for auxiliary systems, such as air conditioning and lighting. Additionally,

MS-SOFCs can be used in remote or off-grid locations, where access to traditional power sources may be limited.

Overall, MS-SOFCs have shown great promise as a technology for clean and efficient power generation. While there are several challenges and limitations that need to be addressed, continued research efforts in materials and device design, as well as advanced manufacturing techniques, can lead to further improvements in the performance, stability, and cost-effectiveness of MS-SOFCs.

8. Conclusions

Metal-supported solid oxide fuel cells represent a promising technology with the potential to address some of the challenges faced by traditional ceramic-supported SOFCs. Recent developments in advanced manufacturing techniques and new materials have shown promise in addressing some of the challenges facing MS-SOFCs. However, MS-SOFCs have developed rapidly and made great strides, but most of them are still in the research stage, and there are still many problems to be explored and solved, for example:

1. The formation of an insulating oxide layer on the metal support during operation, which can decrease cell performance over time, and the need for cathode materials that can operate at lower temperatures.

2. It is necessary to study the internal relationship between the intrinsic properties of the cathode, anode, and electrolyte materials, the microstructure of the battery interface, and the polarization characteristics of the battery, as well as their influence on the SOFC characteristics.

3. The mutual diffusion of Fe, Cr, and Ni between the metal substrate and the anode will lead to a rapid deterioration in the characteristics of SOFC with a metal substrate. Interdiffusion of the Fe-Cr-Ni elements will promote the formation of austenite in the substrate, causing the thermal expansion coefficient of the substrate to change, making it unable to match the thermal expansion characteristics of other components. In addition, the diffusion of the Cr element to the anode will lead to the formation of oxides on the surface of the Ni particles, which will eventually lead to a rapid degradation of the SOFC performance. In addition, the cathode film preparation process still needs to be improved.

4. For MS-SOFC cells in which Fe-based stainless steel is used as a substrate, reduction or joint firing in an inert atmosphere is often used for their preparation to avoid excessive oxidation of the substrate. However, conventional perovskite cathode materials cannot be sufficiently stable under these conditions, and in severe cases, cathode materials may even decompose.

5. One major issue is the compatibility of the metal support with the electrode and electrolyte materials. The high temperatures and corrosive environment in SOFCs can lead to the degradation of the metal support, which can negatively affect the performance and lifespan of the cell. Additionally, the properties of the metal support, such as its thermal expansion coefficient and electrical conductivity, must be carefully matched with those of the other materials in the cell to ensure optimal performance.

6. Another challenge of MS-SOFCs is the thermal expansion mismatch between the metal support and the ceramic materials, such as the electrolyte and the electrodes. This difference in expansion coefficients can lead to mechanical stresses that cause de-lamination, cracking, and failure of the fuel cell. Additionally, the formation of interfacial reactions between the metal support and the ceramic materials can also impair the performance of the fuel cell by creating unwanted compounds that hinder ionic and electronic transport.

In conclusion, MS-SOFCs offer great potential for efficient and sustainable electricity production. However, there are still several problems in MS-SOFC research, as outlined above, to realize their commercial potential. Researchers are actively exploring various approaches to improve the performance and stability of the cell, enhance thermal management, and develop new fabrication and manufacturing techniques. With continued research and development efforts, it is hoped that MS-SOFCs will play an important role in the transition to a clean and sustainable energy future.

Author Contributions: Conceptualization, writing—original draft preparation, writing—review and editing S.O., methodology, formal analysis, investigation and resources, K.K. All authors have read and agreed to the published version of the manuscript.

Funding: The article was prepared as part of the implementation of the scientific project of grant funding for young scientists «Zhas Galym» for 2022–2024 of the Science Committee of the Ministry of Science and Higher Education of the Republic of Kazakhstan AP13268769 «Development and synthesis of a porous metal-ceramic base for thin-film SOFC».

Data Availability Statement: No new data were created.

Conflicts of Interest: The authors declare no conflict of interest.

References

1. Bove, R. Recent trends in fuel cell science and technology. In *Solid Oxide Fuel Cells: Rinciples, Designs and State-of-the-Art in Industries*; Springer: Berlin/Heidelberg, Germany, 2007; pp. 267–285. [CrossRef]
2. Minh, N.Q. Solid oxide fuel cell technology-features and applications. *Solid State Ion.* **2004**, *174*, 271–277. [CrossRef]
3. Singhal, S.C.; Kendall, K. *High-Temperature Solid Oxide Fuel Cells: Fundamentals, Design, and Applications*; Elsevier Advanced Technology: New York, NY, USA, 2003; p. 405.
4. Yamamoto, O. Solid oxide fuel cells: Fundamental aspects and prospects. *Electrochim. Acta.* **2000**, *45*, 2423–2435. [CrossRef]
5. Manohar, A.K.; Narayanan, S.R. Efficient generation of electricity from methane using high temperature fuel cells—status, challenges and prospects. *Isr. J. Chem.* **2014**, *54*, 1443–1450. [CrossRef]
6. Adams, T.A.; Nease, J.; Tucker, D.; Barton, P.I. Energy conversion with solid oxide fuel cell systems: A review of concepts and outlooks for the short and long-term. *Ind. Eng. Chem. Res.* **2013**, *52*, 3089–3111. [CrossRef]
7. Ansar, A.; Szabo, P.; Arnold, J.; Ilhan, Z.; Soysal, D.; Costa, R.; Zagst, A.; Gindrat, M.; Franco, T. Metal supported solid oxide fuel cells and stacks for auxiliary power units-progress, challenges and lessons learned. *ECS Trans.* **2011**, *35*, 147–155. [CrossRef]
8. Kim, K.J.; Park, B.H.; Kim, S.J.; Lee, Y.; Bae, H.; Choi, G.M. Micro solid oxide fuel cell fabricated on porous stainless steel: A new strategy for enhanced thermal cycling ability. *Sci. Rep.* **2016**, *6*, 22443. [CrossRef] [PubMed]
9. Franco, T.; Haydn, M.; Mücke, R.; Weber, A.; Rüttinger, M.; Büchler, O.; Uhlenbruck, S.; Menzler, N.H.; Venskutonis, A.; Sigl, L.S. Development of metal-supported solid oxide fuel cells. *ECS Trans.* **2011**, *35*, 343–349. [CrossRef]
10. Sharaf, O.Z.; Orhan, M.F. An overview of fuel cell technology: Fundamentals and applications. *Renew. Sustain. Energy Rev.* **2014**, *32*, 810–853. [CrossRef]
11. Mougin, J.; Brevet, A.; Grenier, J.C.; Laucournet, R.; Larsson, P.O.; Montinaro, D.; Rodriguez-Martinez, L.M.; Alvarez, M.A.; Stange, M.; Trombert, S. Metal supported solid oxide fuel cells: From materials development to single cell performance and durability tests. *ECS Trans.* **2013**, *57*, 481–490. [CrossRef]
12. Blennow, P.; Hjelm, J.; Klemensø, T.; Ramousse, S.; Kromp, A.; Leonide, A.; Weber, A. Manufacturing and characterization of metal-supported solid oxide fuel cells. *J. Power Sources* **2011**, *196*, 7117–7125. [CrossRef]
13. Tucker, M.C.; Carreon, B.; Charyasatit, J.; Langston, K.; Taylor, C.; Manjarrez, J.; Burton, N.; LaBarbera, M.; Jacobson, C.P. R&D and commercialization of metal-supported SOFC personal power products at point source power. *ECS Trans.* **2013**, *57*, 503–509. [CrossRef]
14. Brandon, N.P.; Blake, A.; Corcoran, D. Development of metal supported solid oxide fuel cells for operation at 500–600 °C. *J. Fuel Cell Sci. Technol.* **2004**, *1*, 61–65. [CrossRef]
15. McKenna, B.J.; Christiansen, N.; Schauperl, R.; Prenninger, P.; Nielsen, J.; Blennow, P.; Klemensø, T.; Ramousse, S.; Kromp, A.; Weber, A. Advances in Metal Supported Cells in the METSOFC EU Consortium. *Fuel Cells* **2013**, *13*, 592–597. [CrossRef]
16. Oishi, N.; Yoo, Y. Fabrication of Cerium Oxide based SOFC having a Porous Stainless Steel Support: Cell Designs, Processing and Performance. *ECS Trans.* **2009**, *25*, 739–744. [CrossRef]
17. Zhou, Y.; Xin, X.; Li, J.; Ye, X.; Xia, C.; Wang, S.; Zhan, Z. Performance and Degradation of Metal-Supported Solid Oxide Fuel Cells with Impregnated Electrodes. *Int. J. Hydrogen Energy* **2014**, *39*, 2279–2285. [CrossRef]
18. Wang, R.; Byrne, C.; Tucker, M.C. Assessment of co-sintering as a fabrication approach for metal-supported proton-conducting solid oxide cells. *Solid State Ion.* **2019**, *332*, 25–33. [CrossRef]
19. Tucker, M.C.; Lau, G.Y.; Jacobson, C.P. Performance of metal-supported SOFCs with infiltrated electrodes. *J. Power Sources* **2007**, *171*, 477–482. [CrossRef]
20. Dogdibegovic, E.; Wang, R.; Lau, G.Y.; Tucker, M.C. Metal-supported solid oxide electrolysis cell (MS-SOEC) with significantly enhanced catalysis. *Energy Technol.* **2019**, *7*, 1801154. [CrossRef]
21. Dogdibegovic, E.; Wang, R.; Lau, G.Y.; Karimaghaloo, A.; Lee, M.H.; Tucker, M.C. Progress in durability of metal-supported solid oxide fuel cells with infiltrated electrodes. *J. Power Sources* **2019**, *437*, 226935. [CrossRef]
22. Kesler, O.; Cuglietta, M.; Harris, J.; Kuhn, J.; Marr, M.; Metcalfe, C. Progress in metal-supported SOFCs using hydrogen and methane fuels. *ECS Trans.* **2013**, *57*, 491–501. [CrossRef]
23. Miyamoto, K.; Kawabata, T.; Tachikawa, Y.; Matsuda, J.; Taniguchi, S.; Matsuzaki, Y.; Hayashi, A.; Sasaki, K. Preparation of Model SOFCs with Proton-conducting electrolyte on metal support using pulse laser deposition. *ECS Trans.* **2021**, *103*, 2033. [CrossRef]

24. Krishnan, V.V. Recent developments in metal-supported solid oxide fuel cells. *Wiley Interdiscip. Rev. 140 Energy Env.* **2017**, *6*, 246–281. [CrossRef]
25. Tucker, M.C. Progress in metal-supported solid oxide fuel cells: A review. *J. Power Sources* **2010**, *195*, 4570–4582. [CrossRef]
26. Tucker, M.C.; Jacobson, C.P.; De Jonghe, L.C.; Visco, S.J. A braze system for sealing metal-supported solid oxide fuel cells. *J. Power Sources* **2006**, *160*, 1049–1057. [CrossRef]
27. Tucker, M.C.; Sholklapper, T.Z.; Lau, G.Y.; De Jonghe, L.C.; Visco, S.J. Progress in metal-supported SOFCs. *ECS Trans.* **2009**, *25*, 673–680. [CrossRef]
28. Antepara, I.; Villarreal, I.; Rodríguez-Martínez, L.M.; Lecanda, N.; Castro, U.; Laresgoiti, A. Evaluation of ferritic steels for use as interconnects and porous metal supports in IT-SOFCs. *J. Power Sources* **2005**, *151*, 103–107. [CrossRef]
29. Matus, Y.B.; De Jonghe, L.C.; Jacobson, C.P.; Visco, S.J. Metal-supported solid oxide fuel cell membranes for rapid thermal cycling. *Solid State Ion.* **2004**, *176*, 443–449. [CrossRef]
30. Haydn, M.; Ortner, K.; Franco, T.; Menzler, N.H.; Venskutonis, A.; Sigl, L.S. Development of Metal-Supported Solid Oxide Fuel Cells Based on a Powder-Metallurgical Manufacturing Route. *Powder Metall.* **2013**, *56*, 382–387. [CrossRef]
31. Rose, L.; Kesler, O.; Decès-Petit, C.; Troczynski, T.; Maric, R. Characterization of porous stainless steel 430 for low and intermediate temperature solid oxide fuel cell (SOFC) substrates. *Int. J. Green Energy* **2009**, *6*, 638–645. [CrossRef]
32. Xia, C.; Liu, Z.; Liu, B.; Ding, D.; Jiang, Z. Development of three-layer intermediate temperature solid oxide fuel cells with direct stainless steel based anodes. *Int. J. Hydrogen Energy* **2012**, *37*, 4401–4405. [CrossRef]
33. Molin, S.; Kusz, B.; Gazda, M.; Jasinski, P. Evaluation of porous 430L stainless steel for SOFC operation at intermediate temperatures. *J. Power Sources* **2008**, *181*, 31–37. [CrossRef]
34. Jablonski, P.D.; Sears, J.S. The impact of alloy chemistry on the formation of a silicon-rich subscale on two classes of ferritic steels. *J. Power Sources* **2013**, *228*, 141–150. [CrossRef]
35. Hwang, C.S.; Tsai, C.H.; Yu, J.F.; Chang, C.L.; Lin, J.M.; Shiu, Y.H.; Cheng, S.W. High Performance Metal-supported Intermediate Temperature Solid Oxide Fuel Cells Fabricated by Atmospheric Plasma Spraying. *J. Power Sources* **2011**, *196*, 1932–1939. [CrossRef]
36. Sarasketa-Zabala, E.; Otaegi, L.; Rodriguez-Martinez, L.M.; Alvarez, M.A.; Burgos, N.; Castro, F. High temperature stability of porous metal substrates under highly humidified hydrogen conditions for metal supported Solid Oxide Fuel Cells. *Solid State Ion.* **2012**, *222*, 16–22. [CrossRef]
37. Bischof, C.; Nenning, A.; Malleier, A.; Martetschlager, L.; Gladbach, A.; Schafbauer, W.; Opitz, A.K.; Bram, M. Microstructure optimization of nickel/gadolinium-doped ceria anodes as key to significantly increasing power density of metal supported solid oxide fuel cells. *Int. J. Hydrogen Energy* **2019**, *44*, 31475–31487. [CrossRef]
38. Yang, S.F.; Shie, Z.J.; Hwang, C.S.; Tsai, C.H.; Chang, C.L.; Huang, T.J.; Lee, R.Y. Ni-Mo porous alloy fabricated as supporting component for metal-supported solid oxide fuel cell and cell performance. *ECS Trans.* **2015**, *68*, 1849–1855. [CrossRef]
39. Wang, X.; Li, K.; Jia, L.; Zhang, Q.; Jiang, S.P.; Chi, B.; Yan, D. Porous Ni-Fe alloys as anode support for intermediate temperature solid oxide fuel cells: I. Fabrication, redox and thermal behaviors. *J. Power Sources* **2015**, *277*, 474–479. [CrossRef]
40. Sadykov, V.A.; Usoltsev, V.V.; Fedorova, Y.E.; Sobyanin, V.A.; Kalinin, P.V.; Arzhannikov, A.V.; Vlasov AYu Korobeinikov, M.V.; Bryazgin, A.A.; Salanov, A.N.; Predtechenskii, M.R.; et al. Design of Medium-Temperature Solid Oxide Fuel Cells on Porous Supports of Deformation Strengthened Ni-Al Alloy. *Russ. J. Electrochem.* **2011**, *47*, 488–493. [CrossRef]
41. Solovyev, A.A.; Rabotkin, S.V.; Shipilova, A.V.; Kirdyashkin, A.I.; Ionov, I.V.; Kovalchuk, A.N.; Maznoy, A.S.; Kitler, V.D.; Borduleva, A.O. Solid Oxide Fuel Cell with Ni-Al Support. *Int. J. Hydrogen Energy* **2015**, *40*, 14077–14084. [CrossRef]
42. Liu, M.; Finlayson, T.R.; Smith, T.F.; Tanner, L.E. Martensite precursor observations using thermal expansion: Ni-Al. *Mater. Sci. Eng.* **1992**, *157*, 225–232. [CrossRef]
43. Johnson, J.; Qu, J. Effective modulus and coefficient of thermal expansion of Ni-YSZ porous cermets. *J. Power Sources* **2008**, *181*, 85–92. [CrossRef]
44. Windes, W.E.; Zuck, L.D.; Shaber, E.L.; Erickson, A.E.; Lessing, P.A. A Low TEC Intermetallic bipolar plate. *Proc. Electrochem. Soc.* **2003**, *7*, 879–887. [CrossRef]
45. Cowin, P.I.; Petit, C.T.; Lan, R.; Irvine, J.T.; Tao, S. Recent progress in the development of anode materials for solid oxide fuel cells. *Adv. Energy Mater.* **2011**, *1*, 314–332. [CrossRef]
46. Medvedev, D.A.; Lyagaeva, J.G.; Gorbova, E.V.; Demin, A.K.; Tsiakaras, P. Advanced materials for SOFC application: Strategies for the development of highly conductive and stable solid oxide proton electrolytes. *Prog. Mater. Sci.* **2016**, *75*, 38–79. [CrossRef]
47. Nielsen, J.; Persson, Å.H.; Sudireddy, B.R.; Irvine, J.T.; Thydén, K. Infiltrated $La_{0.4}Sr_{0.4}Fe_{0.03}Ni_{0.03}Ti_{0.94}O_3$ based anodes for all ceramic and metal supported solid oxide fuel cells. *J. Power Sources* **2017**, *372*, 99–106. [CrossRef]
48. Haydn, M.; Ortner, K.; Franco, T.; Uhlenbruck, S.; Menzler, N.H.; Stöver, D. Multi-layer thin-film electrolytes for metal supported solid oxide fuel cells. *J. Power Sources* **2014**, *256*, 52–60. [CrossRef]
49. Paek, J.Y.; Chang, I.; Park, J.H.; Ji, S.; Cha, S.W. A study on properties of yttrium stabilized zirconia thin films fabricated by different deposition techniques. *Renew. Energy* **2014**, *65*, 202–206. [CrossRef]
50. Zhan, Z.; Zhou, Y.; Wang, S.; Liu, X.; Meng, X.; Wen, T. Nanostructure Electrodes for Metal-Supported Solid Oxide Fuel Cells. *ECS Trans.* **2013**, *57*, 925–931. [CrossRef]
51. Liu, X.; Han, D.; Zhou, Y.; Meng, X.; Wu, H.; Li, J.; Zeng, F.; Zhan, Z. Sc-substituted $Ln_{0.6}Sr_{0.4}FeO_{3-\delta}$ mixed conducting oxides as promising electrodes for symmetrical solid oxide fuel cells. *J. Power Sources* **2014**, *15*, 457–463. [CrossRef]

52. Zhou, Y.; Zhan, Z.; Wang, S. Metal-Supported Solid Oxide Fuel Cells with Impregnated Electrodes. *ECS Trans.* **2013**, *57*, 877–883. [CrossRef]
53. Sudireddy, B.R.; Nielsen, J.; Thydén KT, S.; Persson, A.H.; Brodersen, K. Investigation of Novel Electrocatalysts for Metal Supported Solid Oxide Fuel Cells–Ru:GDC. *ECS Trans.* **2015**, *68*, 1417–1426. [CrossRef]
54. Kim, K.J.; Kim, S.J.; Choi, G.M. Y0.08Sr0.88TiO3-CeO2 composite as a diffusion barrier layer for stainless-steel supported solid oxide fuel cell. *J. Power Sources* **2016**, *307*, 385–390. [CrossRef]
55. Tucker, M.C. Progress in metal-supported solid oxide electrolysis cells: A review. *Int. J. Hydrogen Energy* **2020**, *45*, 24203–24218. [CrossRef]
56. Thaler, F.; Nenning, A.; Bischof, C.; Udomsilp, D.; de Haart, L.G.J.; Opitz, A.K.; Bram, M. Optimized Cell Processing as the Key of High Electrochemical Performance of Metal Supported Solid Oxide Fuel Cells. *ECS Trans.* **2019**, *91*, 887–900. [CrossRef]
57. Liu, J.; Briss, V.; Hill, J. Electrochemical performance and microstructure characterization of nickel yttrium-stabilized zirconia anode. *AIChE J.* **2010**, *56*, 1651–1656. [CrossRef]
58. Singhal, S.C. Advances in solid oxide fuel cell technology. *Solid State Ion.* **2000**, *135*, 305–313. [CrossRef]
59. Goodenough, J.B.; Huang, Y.H. Alternative anode materials for solid oxide fuel cells. *J. Power Sources* **2007**, *173*, 1–10. [CrossRef]
60. Koide, H.; Someya, Y.; Yoshida, T.; Maruyama, T. Properties of Ni/YSZ cermet as anode for SOFC. *Solid State Ion.* **2001**, *132*, 253–260. [CrossRef]
61. Zhou, Y.; Zhang, Z.; Yuan, C.; Li, J.; Xia, C.; Zhan, Z.; Wang, S. Metal-supported solid oxide fuel cells with in-situ sintered $(Bi_2O_3)_{0.7}(Er_2O_3)_{0.3}$-Ag composite cathode. *Int. J. Hydrogen Energy* **2013**, *38*, 16579–16583. [CrossRef]
62. Udomsilp, D.; Thaler, F.; Menzler, N.H.; Bischof, C.; de Haart, L.G.J.; Opitz, A.K.; Guillon, O.; Bram, M. Dual-Phase Cathodes for Metal-Supported Solid Oxide Fuel Cells: Processing, Performance, Durability. *J. Electrochem. Soc.* **2019**, *166*, F506–F510. [CrossRef]
63. Jordan, N.; Assenmacher, W.; Uhlenbruck, S.; Haanappel, V.A.C.; Buchkremer, H.P.; Stöver, D.; Mader, W. Ce0.8Gd0.2O2−δ protecting layers manufactured by physical vapor deposition for IT-SOFC. *Solid State Ionics.* **2008**, *179*, 919–923. [CrossRef]
64. Fergus, J.W. Electrolytes for solid oxide fuel cells. *J. Power Sources* **2006**, *162*, 30–40. [CrossRef]
65. Badwal, S.P. Oxygen-ion conducting electrolyte materials for solid oxide fuel cells. *Ionics* **2000**, *6*, 1–21. [CrossRef]
66. Zhou, Y.; Yuan, C.; Chen, T.; Meng, X.; Ye, X.; Li, J. Evaluation of Ni and Ni-$Ce_{0.8}Sm_{0.2}O_{2-\delta}$ (SDC) impregnated 430L anodes for metal-supported solid oxide fuel cells. *J. Power Sources* **2014**, *267*, 117–122. [CrossRef]
67. Ralph, J.M. Materials for lower temperature solid oxide fuel cell. *J. Mater. Sci.* **2001**, *36*, 1161–1172. [CrossRef]
68. Tsipis, E.V.; Kharton, V.V. Electrode materials and reaction mechanisms in solid oxide fuel cells: A brief review. III. Recent trends and selected methodological aspects. *J. Solid State Electrochem.* **2011**, *15*, 1007–1040. [CrossRef]
69. Figueiredo, F.M.; Marques, M.B. Electrolytes for Solid Oxide Fuel Cellls. *WREs Energy Environ.* **2013**, *2*, 52–72. [CrossRef]
70. Molin, S.; Tolczyk, M.; Gazda, M.; Jasinski, P. Stainless steel yttria stabilized zirconia composite supported solid oxide fuel cell. *J. Fuel Cell Sci. Technol.* **2011**, *8*, 1–5. [CrossRef]
71. Kasyanova, A.V.; Zvonareva, I.A.; Tarasova, N.A.; Bi, L.; Medvedev, D.A.; Shao, Z. Electrolyte materials for protonic ceramic electrochemical cells: Main limitations and potential solutions. *Mater. Rep. Energy* **2022**, *2*, 100158. [CrossRef]
72. Cervera, R.B.; Oyama, Y.; Miyoshi, S.; Oikawa, I.; Takamura, H.; Yamaguchi, S. Nanograined Sc-doped $BaZrO_3$ as a proton conducting solid electrolyte for intermediate temperature solid oxide fuel cells (IT-SOFCs). *Solid State Ion.* **2014**, *264*, 1–6. [CrossRef]
73. Zając, W.; Rusinek, D.; Zheng, K.; Molenda, J. Applicability of Gd-doped $BaZrO_3$, $SrZrO_3$, $BaCeO_3$ and $SrCeO_3$ proton conducting perovskites as electrolytes for solid oxide fuel cells. *Open Chem.* **2013**, *11*, 471–484. [CrossRef]
74. Qu, E.; Hao, X.; Xiao, M.; Han, D.; Huang, S.; Huang, Z.; Meng, Y. Proton exchange membranes for high temperature proton exchange membrane fuel cells: Challenges and perspectives. *J. Power Sources* **2022**, *533*, 231386. [CrossRef]
75. Selim, A.; Szijjártó, G.P.; Románszki, L.; Tompos, A. Development of WO_3–Nafion Based Membranes for Enabling Higher Water Retention at Low Humidity and Enhancing PEMFC Performance at Intermediate Temperature Operation. *Polymers* **2022**, *14*, 2492. [CrossRef] [PubMed]
76. Zhou, Y.; Meng, X.; Liu, X.; Pan, X.; Li, J.; Ye, X. Novel architectured metal-supported solid oxide fuel cells with Mo-doped $SrFeO_{3-\delta}$ electrocatalysts. *J. Power Sources* **2014**, *267*, 128–135. [CrossRef]
77. Klemensø, T.; Nielsen, J.; Blennow, P.; Persson, A.H.; Stegk, T.; Christensen, B.H. High performance metal-supported solid oxide fuel cells with Gd-doped ceria barrier layers. *J. Power Sources* **2011**, *196*, 9459–9466. [CrossRef]
78. Franco, T.; Schibinger, K.; Ilhan, Z.; Schiller, G.; Venskutonis, A. Ceramic Diffusion Barrier Layers for Metal Supported SOFCs. *ECS Trans.* **2007**, *7*, 771–780. [CrossRef]
79. Rüttinger, M.; Mücke, R.; Franco, T.; Büchler, O.; Menzler, N.H.; Venskutonis, A. Metal-Supported Cells with Comparable Performance to Anode-Supported Cells in Short-Term Stack Environment. *ECS Trans.* **2011**, *35*, 259–268. [CrossRef]
80. Macwan, A.; Chen, D.L.; Marr, M.; Kesler, O. Residual stresses in suspension plasma sprayed electrolytes in metal-supported solid oxide fuel half cells. *J. Power Sources* **2013**, *221*, 397–405. [CrossRef]
81. Gelfond, N.V.; Bobrenok, O.F.; Predtechensky, M.R.; Morozova, N.B.; Zherikova, K.V.; Igumenov, I.K. Chemical vapor deposition of thin films of electrolytes based on zirconium oxide stabilized with yttrium oxide. *Inorg. Mater.* **2009**, *45*, 718–725. [CrossRef]
82. Szabo, P.; Arnold, J.; Franco, T.; Gindrat, M.; Refke, A.; Zagst, A.; Ansar, A. Progress in the Metal Supported Solid Oxide Fuel Cells and Stacks for APU. *ECS Trans.* **2009**, *25*, 175–185. [CrossRef]

83. Kurokawa, H.; Lau, G.Y.; Jacobson, C.P.; De Jonghe, L.C.; Visco, S.J. Water-based binder system for SOFC porous steel substrate. *J. Mater. Porc. Technol.* **2007**, *182*, 469–4760. [CrossRef]
84. Yoon, S.P. Performance of anode-supported solid oxide fuel cell with $La_{0.85}Sr_{0.15}MnO_3$ cathode modified by sol-gel coating technique. *J. Power Sources* **2002**, *106*, 160–166. [CrossRef]
85. Sønderby, S.; Aijaz, A.; Helmersson, U.; Sarakinos, K.; Eklund, P. Deposition of yttria-stabilized zirconia thin films by high power impulse magnetron sputtering and pulsed magnetron sputtering. *Surf. Coat. Technol.* **2014**, *240*, 1–6. [CrossRef]
86. Rodriguez-Martinez, L.M.; Otaegi, L.; Alvarez, M.; Rivas, M.; Gomez, N.; Zabala, A.; Arizmendiarrieta, I.; Antepara, A.; Urriolabeitia, M.; Olave, I.; et al. Degradation Studies on Tubular Metal Supported SOFC Cell Designs, Processing and Performance. *ECS Trans.* **2009**, *25*, 745–752. [CrossRef]
87. Sun, C.; Hui, R.; Roller, J. Cathode materials for solid oxide fuel cells: A review. *J. Solid State Electrochem.* **2010**, *14*, 1125–1144. [CrossRef]
88. Richter, J.; Holtappels, P.; Graule, T.; Nakamura, T.; Gauckler, L.J. Materials design for perovskite SOFC cathodes. *Mon. Chem. Chem. Mon.* **2009**, *140*, 985–999. [CrossRef]
89. Zhou, Y.; Liu, X.; Li, J.; Nie, H.; Ye, X.; Wang, S.; Zhan, Z. Novel metal-supported solid oxide fuel cells with impregnated symmetric $La_{0.6}Sr_{0.4}Fe_{0.9}Sc_{0.1}O_{3-d}$ electrodes. *J. Power Sources* **2014**, *252*, 164–168. [CrossRef]
90. Zhou, Y.; Han, D.; Yuan, C.; Liu, M.; Chen, T.; Wang, S. Infiltrated $SmBa_{0.5}Sr_{0.5}Co_2O_{5+\delta}$ cathodes for metal-supported solid oxide fuel cells. *Electrochim. Acta* **2014**, *149*, 231–236. [CrossRef]
91. Yu, R. Quantitative assessment of anode contribution to cell degradation under various polarization conditions using industrial size planar solid oxide fuel cells. *Int. J. Hydrogen Energy* **2018**, *43*, 2429–2435. [CrossRef]
92. Kim, S.H. Effect of Water Vapor and SOx in Air on the Cathodes of Solid Oxide Fuel Cells. Symposium R–Life-Cycle Analysis for New Energy Conversion and Storage Systems. *MRS Online Proc. Libr.* **2007**, *1041*, R03–R10. [CrossRef]
93. Baek, S.W.; Jeong, J.; Kim, Y.M.; Kim, J.H.; Shin, S.; Bae, J. Metal-supported solid oxide fuel cells with barium-containing in-situ cathodes. *Solid State Ion.* **2011**, *192*, 387–393. [CrossRef]
94. Sahu, N.; Parija, B.; Panigrahi, S. Fundamental understanding and modeling of spin coating process: A review. *Indian J. Phys.* **2009**, *83*, 493–502. [CrossRef]
95. Kim, Y.-M.; Kim-Lohsoontorn, P.; Bae, J. Effect of unsintered gadolinium-doped ceria buffer layer on performance of metal-supported solid oxide fuel cells using unsintered barium strontium cobalt ferrite cathode. *J. Power Sources* **2010**, *195*, 64207. [CrossRef]
96. Han, D.; Wu, H.; Li, J.; Wang, S.; Zhan, Z. Nanostructuring of $SmBa_{0.5}Sr_{0.5}Co_2O_{5+\delta}$ cathodes for reduced-temperature solid oxide fuel cells. *J. Power Sources* **2014**, *246*, 409–416. [CrossRef]
97. Ni, D.W.; Esposito, V. Densification of $Ce_{0.9}Gd_{0.1}O_{1.95}$ barrier layer by in-situ solid state reaction. *J. Power Sources* **2014**, *266*, 393–400. [CrossRef]
98. Sønderby, S.; Klemensø, T.; Christensen, B.H.; Almtoft, K.P.; Lu, J.; Nielsen, L.P.; Eklund, P. Magnetron sputtered gadolinia-doped ceria diffusion barriers for metal supported solid oxide fuel cells. *J. Power Sources* **2014**, *267*, 452–458. [CrossRef]
99. Shen, Y. Preparation of Nanocomposite GDC/LSCF Cathode Material for IT-SOFC by Induction Plasma Spraying. *J. Therm. Spray Technol.* **2011**, *20*, 145–153. [CrossRef]
100. Blennow, P.; Klemensø, T.; Nielsen, J.; Persson, A.H.; Stegk, T.; Hjalmarsson, P. Development of Long-term Stable and High-performing Metal-supported SOFCs. *ECS Trans.* **2011**, *35*, 369–378. [CrossRef]
101. Bae, J.; Lee, C. Fabrication and characterization of metal-supported solid oxide fuel cells. *J. Power Sources* **2008**, *176*, 62–69. [CrossRef]
102. Li, J. High-performance and stable $La_{0.8}Sr0_2Fe_{0.9}Nb_{0.1}O_{3-\delta}$ anode for direct carbon solid oxide fuel cells fueled by activated carbon and corn straw derived carbon. *Int. J. Hydrogen Energy* **2018**, *43*, 12358–12367. [CrossRef]
103. Hagen, A. Effect of Humidity in Air on Performance and Long-Term Durability of SOFCs. *ECS Trans.* **2009**, *25*, 439–446. [CrossRef]
104. Nielsen, J. Effect of cathode gas humidification on performance and durability of Solid Oxide Fuel Cells. *Solid State Ion.* **2010**, *181*, 517–524. [CrossRef]
105. Yang, Z. A short review of cathode poisoning and corrosion in solid oxide fuel cell. *Int. J. Hydrogen Energy* **2017**, *42*, 24948–24959. [CrossRef]
106. Li, Y.; Xie, Y.; Gong, J.; Chen, Y.; Zhang, Z. Preparation of Ni/YSZ materials for SOFC anodes by buffer-solution method. *Mater. Sci. Eng. B* **2001**, *86*, 119–122. [CrossRef]
107. Bronin, D. Nature of Electrode Degradation in SOFCs. In Proceedings of the 8th European Solid Oxide Fuel Cell Forum, Lucerne, Switzerland, 30 June–3 July 2008; p. B1001.
108. Hagen, A. Degradation of anode supported SOFCs as a function of temperature and current load. *J. Electrochem. Soc.* **2006**, *153*, A1165–A1171. [CrossRef]
109. He, Z. Cyclic polarization enhances the operating stability of $La_{0.57}Sr_{0.38}Co_{0.18}Fe_{0.72}Nb_{0.1}O_{3-\delta}$ oxygen electrode of reversible solid oxide cells. *J. Power Sources* **2018**, *404*, 73–80. [CrossRef]
110. Hilpert, K.; Das, D.; Miller, M.; Peck, D.H.; Weiß, R. Chromium vapor species over solid oxide fuel cell interconnect materials and their potential for degradation processes. *J. Electrochem. Soc.* **1996**, *143*, 3642–3647. [CrossRef]
111. Williams, M.C. Solid Oxide Fuel Cells: Fundamentals to Systems. *Fuel Cells* **2007**, *1*, 78–85. [CrossRef]

112. Simwonis, D. Nickel coarsening in annealed Ni/8YSZ anode substrates for solid oxide fuel cells. *Solid State Ion.* **2000**, *132*, 241–251. [CrossRef]
113. Tanasini, P. Experimental and theoretical investigation of degradation mechanisms by particle coarsening in SOFC Electrodes. *Fuel Cells* **2009**, *9*, 740–752. [CrossRef]
114. Jiang, S.P. Sintering behavior of Ni/Y_2O_3-ZrO_2 cermet electrodes of solid oxide fuel. *J. Mater. Sci.* **2003**, *38*, 3775–3782. [CrossRef]
115. Matsui, T. Comparative study on performance stability of Ni–oxide cermet anodes under humidified atmospheres in solid oxide fuel cells. *J. Electrochem. Soc.* **2012**, *159*, F456–F460. [CrossRef]
116. Faes, A. Nickel–zirconia anode degradation and triple phase boundary quantification from microstructural analysis. *Fuel Cells* **2009**, *9*, 841–851. [CrossRef]
117. Pihlatie, M.H. Electrical conductivity of Ni–YSZ composites: Degradation due to Ni particle growth. *Solid State Ion.* **2011**, *189*, 82–90. [CrossRef]
118. De Angelis, S.; Jørgensen, P.S.; Tsai, E.H.; Holler, M.; Kreka, K.; Bowen, J.R. Three dimensional characterization of nickel coarsening in solid oxide cells via ex-situ ptychographic nano-tomography. *J. Power Sources* **2018**, *383*, 72–79. [CrossRef]
119. Kim, Y.-M.; Bae, J. Investigation of mixed conducting cathode for metal-supported SOFC. In Proceedings of the ASME 2009 7th International Conference on Fuel Cell Science, Engineering and Technology, Newport Beach, CA, USA, 8–10 June 2009; pp. 847–849. [CrossRef]
120. Joo, J.H.; Choi, G.M. Simple fabrication of micro-solid oxide fuel cell supported on metal substrate. *J. Power Sources* **2008**, *182*, 589–593. [CrossRef]
121. Park, Y.M.; Kim, J.H.; Kim, H. Effects of a current treatment for an in-situ sintered cathode in a Ni-supported solid oxide fuel cell. *Int. J. Hydrogen Energy* **2012**, *37*, 555–565. [CrossRef]
122. Esposito, V.; Traversa, E.; Wachsman, E.D. Pb2Ru2O6.5 as a low-temperature cathode for bismuth oxide electrolytes. *J. Electrochem. Soc.* **2005**, *152*, A2300–A2305. [CrossRef]
123. Tsai, C.H.; Hwang, C.S.; Chang, C.L.; Wu, S.H.; Lin, H.H.; Shiu, W.H.; Lin, J.K.; Yang, S.F.; Fu, C.Y.; Yang, C.S. Performances of plasma sprayed metal-supported solid oxide fuel cell and stack. *Fuel Cells* **2018**, *18*, 800–808. [CrossRef]
124. Baek, S.W.; Jeong, J.; Kim, J.H.; Lee, C.; Bae, J. Interconnect-integrated solid oxide fuel cell with high temperature sinter-joining process. *Int. J. Hydrogen Energy* **2010**, *35*, 11878–11889. [CrossRef]
125. Shen, F.; Wang, R.; Tucker, M.C. Long term durability test and post mortem for metal-supported solid oxide electrolysis cells. *J. Power Sources* **2020**, *474*, 228618. [CrossRef]
126. Lee, K.; Kang, J.; Lee, J.; Lee, S.; Bae, J. Evaluation of metal-supported solid oxide fuel cells (MS-SOFCs) fabricated at low temperature (∼1000 °C) using wet chemical coating processes and a catalyst wet impregnation method. *Int. J. Hydrogen Energy* **2018**, *43*, 3786–3796. [CrossRef]
127. Choi, J.-J.; Lee, J.-H.; Park, D.-S.; Hahn, B.-D.; Yoon, W.-H.; Lin, H.-T. Oxidation Resistance Coating of LSM and LSCF on SOFC Metallic Interconnects by the Aerosol Deposition Process. *J. Am. Ceram. Soc.* **2007**, *90*, 1926–1929. [CrossRef]
128. Konysheva, E.; Penkalla, H.; Wessel, E.; Mertens, J.; Seeling, U.; Singheiser, L.; Hilpert, K. Chromium poisoning of perovskite cathodes by the ODS alloy Cr5Fe1Y2O3 and the high chromium ferritic steel Crofer22APU. *J. Electrochem. Soc.* **2006**, *153*, A765–A773. [CrossRef]
129. Talic, B.; Falk-Windisch, H.; Venkatachalam, V.; Hendriksen, P.V.; Wiik, K.; Lein, H.L. Effect of coating density on oxidation resistance and Cr vaporization from solid oxide fuel cell interconnects. *J. Power Sources* **2017**, *354*, 57–67. [CrossRef]
130. Roehrens, D.; Packbier, U.; Fang, Q.; Blum, L.; Sebold, D.; Bram, M.; Menzler, N. Operation of Thin-Film Electrolyte Metal-Supported Solid Oxide Fuel Cells in Lightweight and Stationary Stacks: Material and Microstructural Aspects. *Materials* **2016**, *9*, 762. [CrossRef]
131. Brandner, M.; Bram, M.; Froitzheim, J.; Buchkremer, H.P.; Stöver, D. Electrically Conductive diffusion barrier layers for metal-supported SOFC. *Solid State Ion.* **2008**, *179*, 1501–1504. [CrossRef]
132. Brylewski, T.; Nanko, M.; Maruyama, T.; Przybylski, K. Application of Fe-16Cr ferritic alloy to interconnector for a solid oxide fuel cell. *Solid State Ion.* **2001**, *143*, 131–150. [CrossRef]
133. Yang, Z.; Hardy, J.S.; Walker, M.S.; Xia, G.; Simner, S.P.; Stevenson, J.W. Structure and conductivity of thermally grown scales on ferritic Fe-Cr-Mn steel for SOFC interconnect application. *J. Electrochem. Soc.* **2004**, *151*, A1825. [CrossRef]
134. Bertoldi, M.; Zandonella, T.; Montinaro, D.; Sglavo, V.M.; Fossati, A.; Lavacchi, A.; Giolli, C.; Bardi, U. Protective coatings of metallic interconnects for IT-SOFC application. *J. Fuel Cell Sci. Technol.* **2008**, *5*, 011001. [CrossRef]
135. Mineshige, A.; Fukushima, K.; Okada, S.; Kikuchi, T.; Kobune, M.; Yazawa, T.; Kikuchi, K.; Inaba, M.; Ogumi, Z. Porous Metal Tubular Support for Solid Oxide Fuel Cell Design. *Electrochem. Solid-State Lett.* **2006**, *9*, A427–A429. [CrossRef]
136. Li, K.; Wang, X.; Jia, L.; Yan, D.; Pu, J.; Chi, B.; Jian, L. High performance Ni–Fe alloy supported SOFCs fabricated by low cost tape casting-screen printing-cofiring process. *Int. J. Hydrogen Energy* **2014**, *39*, 19747–19752. [CrossRef]
137. Wei, P.; Sofie, S.; Zhang, Q.; Petric, A. Metal Supported Solid Oxide Fuel Cell by Freeze Tape Casting. *ECS Trans.* **2011**, *35*, 379–383. [CrossRef]
138. Grabke, H.J. Oxidation of NiAl and FeAl. *Intermetallics* **1999**, *7*, 1153–1158. [CrossRef]
139. Wang, Z.; Tian, W.; Li, X. Oxidation behavior of NiAl nanoparticles prepared by hydrogen plasma-metal reaction. *Mater. Chem. Phys.* **2008**, *107*, 381–384. [CrossRef]

140. Kim, S.H.; Oh, M.H.; Kishida, K.; Hirano, T.; Wee, D.M. Deposition of NiAl coating for improvement of oxidation resistance of cold-rolled Ni3Al foils. *Intermetallics* **2005**, *13*, 129–136. [CrossRef]
141. Windes, W.E.; Smith, C.; Wendt, D.; Erickson, A.; Walraven, J.; Lessing, P.A. Electrode coatings for high temperature hydrogen electrolysis. *J. Mater. Sci.* **2007**, *42*, 2717–2723. [CrossRef]
142. Promsen, M.; Komatsu, Y.; Sciazko, A.; Kaneko, S.; Shikazono, N. Feasibility study on saturated water cooled solid oxide fuel cell stack. *Appl. Energy* **2020**, *279*, 115803. [CrossRef]
143. Zeng, Z.; Qian, Y.; Zhang, Y.; Hao, C.; Dan, D.; Zhuge, W. A review of heat transfer and thermal management methods for temperature gradient reduction in solid oxide fuel cell (SOFC) stacks. *Appl. Energy* **2020**, *280*, 115899. [CrossRef]
144. Thaler, F.; Udomsilp, D.; Schafbauer, W.; Bischof, C.; Fukuyama, Y.; Miura, Y.; Kawabuchi, M.; Taniguchi, S.; Takemiya, A.; Nenning, A.K. Redox Stability of Metal Supported Fuel Cells with Nickel/Gadolinium-Doped Ceria Anode. *J. Power Sources* **2019**, *434*, 226751. [CrossRef]
145. Sudireddy, B.R.; Nielsen, J.; Persson, Å.H.; Thydén, K.; Brodersen, K.; Ramousse, S.; Neagu, D.; Stefan, E.; Irvine, J.T.S.; Geisler, H.; et al. Development of robust metal-supported SOFCs and stack components in EU METSAPP Consortium. *Fuel Cells* **2017**, *17*, 508–516. [CrossRef]
146. Leah, R.T.; Bone, P.A.; Selcuk, A.; Rahman, M.; Clare, A.; Lankin, M.; Felix, F.; Mukerjee, S.; Selby, M.A. Latest results and commercialization of the ceres power steelCell®technology platform. *ECS Trans.* **2019**, *91*, 51–61. [CrossRef]
147. Gao, J.T.; Li, J.H.; Wang, Y.P.; Li, C.J.; Li, C.X. Self-Sealing Metal-Supported SOFC Fabricated by Plasma Spraying and Its Performance under Unbalanced Gas Pressure. *J. Therm. Spray Technol.* **2020**, *29*, 2001–2011. [CrossRef]